ANALYSIS OF DELAMINATION

Frank W. Crossman
Lockheed Palo Alto Research Laboratory
Lockheed Missiles and Space Company, Inc.
Palo Alto, California

INTRODUCTION

This paper reviews our understanding of the influence of delamination on the fracture sequence and final fracture of graphite-epoxy laminates. The emphasis here is on tensile fracture.

The paper is organized as follows:

(1) Review of the common fracture modes in laminates and their interaction (based on Lockheed and NASA studies)

(2) Review of free-edge stress analysis and prediction of delamination sites (based on studies by Lockheed Palo Alto Research Laboratory and Drexel University)

(3) Consideration of the problem of predicting delamination fracture in regions containing a high stress gradient (based on studies by Lockheed for NASA)

(4) Analysis of delamination fracture by calculation of strain energy release rate (based on studies by Drexel University and Lockheed)

(5) Consideration of the interaction of interlaminar and intralaminar fracture (based on studies by Drexel University and Lockheed for the Air Force Office of Scientific Research)

(6) Analysis of the interrelationship between strength and stiffness (based on studies by Lockheed for NASA)

(7) Consideration of the correlation between strain energy analysis and statistical analysis approaches in predicting the criticality of a laminate crack (based on studies by Lockheed, Cornell University, and Drexel University)

The following people contributed to the observations, analysis methods, and methodology of delamination fracture analysis described in this paper: J. G. Bjeletich and W. J. Warren (Lockheed Palo Alto), A. S. D. Wang and G. E. Law (Drexel University), T. K. O'Brien (NASA Langley), and J. T. Ryder (Lockheed Rye Canyon). Finally, many researchers have contributed to the understanding of delamination and its influence on laminate fracture. These people are acknowledged in the partial bibliography at the end of this paper.

Five cases that involve delamination fracture are presented. These are:

(1) Free-edge delamination

(2) Compression delamination

(3) Delamination interaction with intralaminar cracking

    (a) Ply peeling

    (b) Delamination after transverse cracking

    (c) Simultaneous delamination/transverse cracking

These cases are illustrated in the five figures which follow.

INTERLAMINAR FRACTURE - CASE 1 : FREE EDGE PLY DELAMINATION

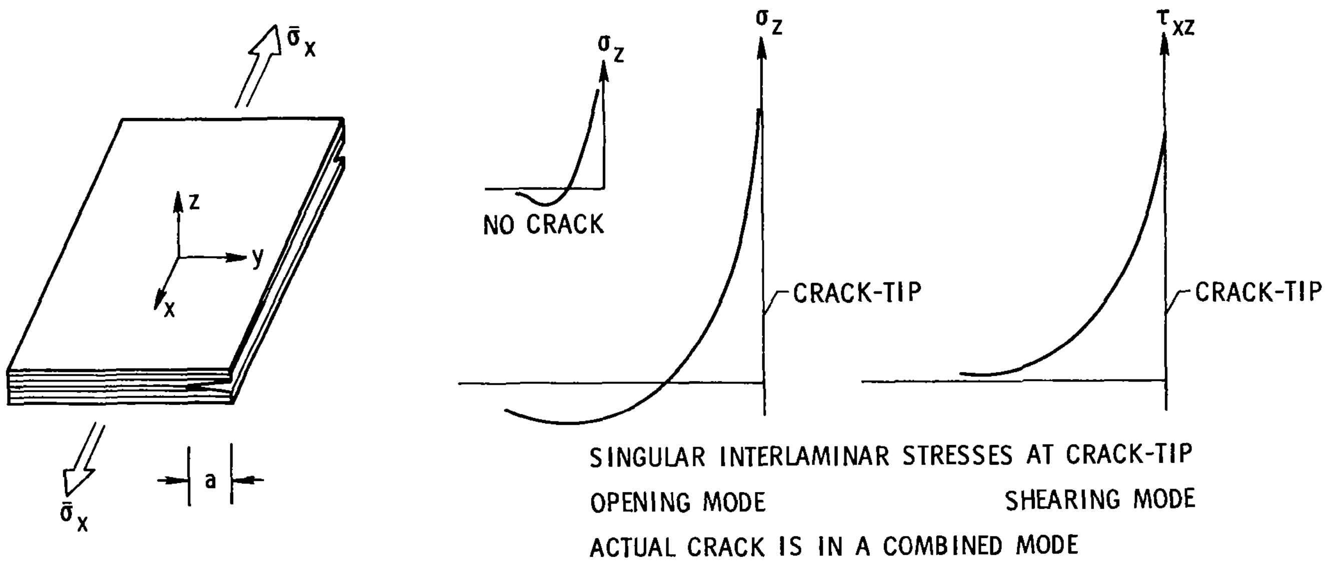

SINGULAR INTERLAMINAR STRESSES AT CRACK-TIP

OPENING MODE   SHEARING MODE

ACTUAL CRACK IS IN A COMBINED MODE

INTERLAMINAR FRACTURE - CASE 2: COMPRESSIVE LAMINATE FAILURE MECHANISMS

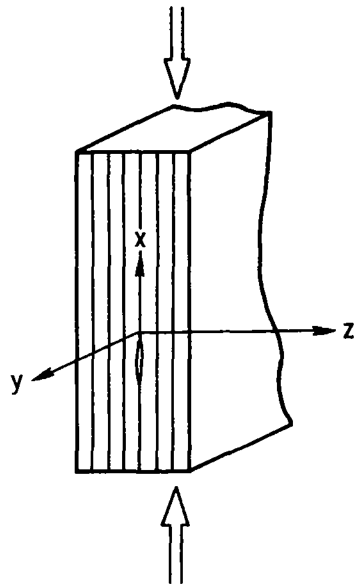

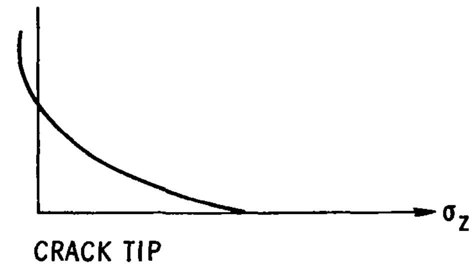

SINGULAR INTERLAMINAR CRACK TIP NORMAL STRESS

CRACK GROWTH IS PRECIPITATED BY STRUCTURAL BUCKLING ACTION

UNSTABLE CRACK GROWTH DETERMINES THE COMPRESIVE STRENGTH OF LAMINATE

INTERLAMINAR FRACTURE - CASE 3 (a): PLY-PEELING (ALSO A CASE OF PLY DELAMINATION) (SURFACE DELAMINATION)

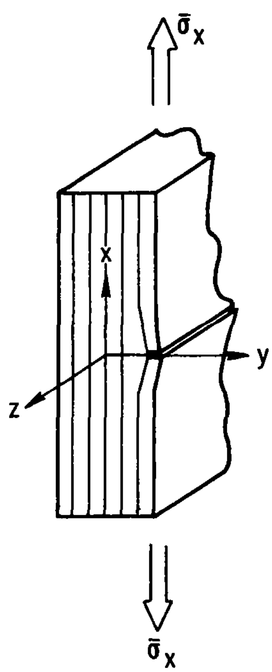

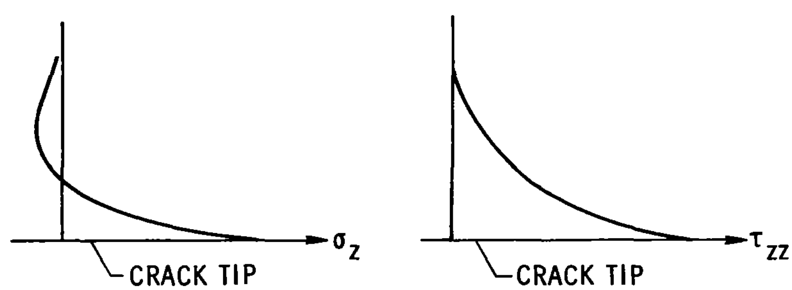

SINGULAR INTERLAMINAR STRESSES AT CRACK TIP

OPENING MODE SHEARING MODE

ACTUAL CRACK IS IN A COMBINED MODE

INTERLAMINAR FRACTURE - CASE 3(b):

*FREE EDGE DELAMINATION (ALONG 25/90 PLANE, MIXED MODE)

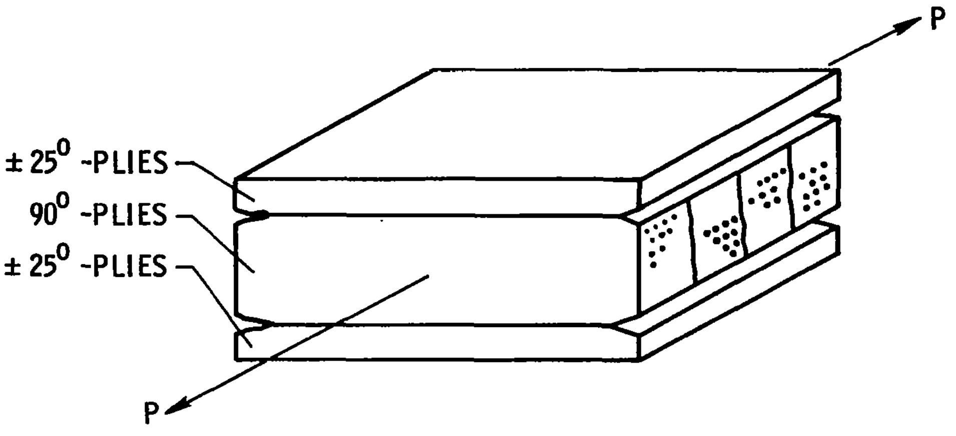

INTERLAMINAR FRACTURE - CASE 3(c):

*DELAMINATION EMANATING FROM THE ROOT OF A TRANSVERSE CRACK (MIXED MODE)

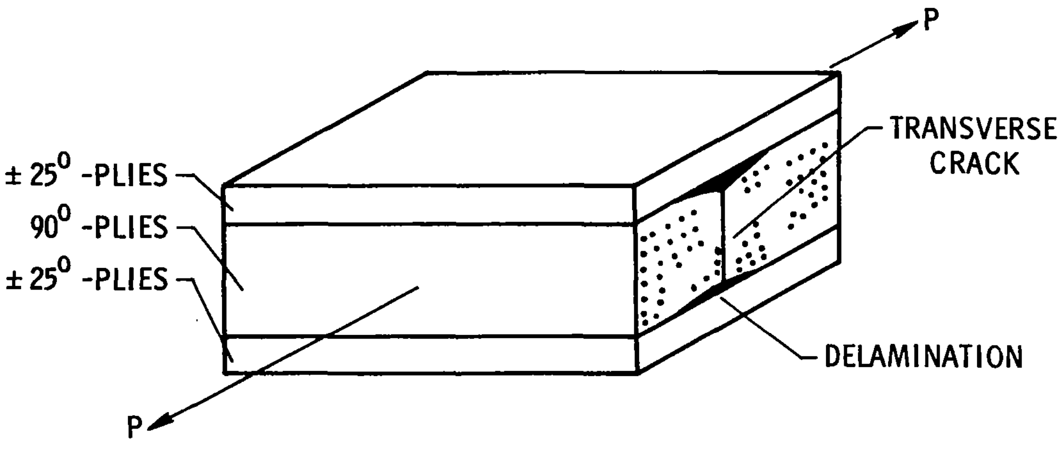

ULTIMATE TENSILE STRENGTH VERSUS STACKING SEQUENCE

Studies were conducted in the mid-1970's to examine the influence of laminate stacking sequence on the tensile properties. The results shown below and in the next figure compare the ultimate strengths of a number of quasi-isotropic laminates constructed of T300/934 tape and fabric (ref. 1). A large variation in strength was found. This variation was not predicted from laminated plate analysis where stacking sequence does not alter the in-plane ply stresses when the specimen is loaded under tension.

TENSILE STRENGTH OF QUASI-ISOTROPIC T300/934 LAMINATES AS A FUNCTION OF PLY STACKING SEQUENCE (LAMINATES DESIGNATED HMF WERE FABRICATED FROM WOVEN GRAPHITE FABRIC)

{From ref. 1}

MATERIAL	THICKNESS (IN.)	PANEL NO.	LAYUP SEQUENCE
T300/934	0.042	13	$[0/+45/-45/90]_s$
T300/934	0.042	15	$[90/45/-45/0]_s$
T300/934	0.042	14	$[0/90/45/-45]_s$
T300/934	0.042	17	$[90/0/45/-45]_s$
HMF330C/34	0.054	2	$[(0/90)/(\pm45)]_s$
HMF330C/34	0.108	4	$[(0/90)/(90/0)/(\pm45)/(\mp45)]_s$
T300/934	0.042	18	$[45/-45/90/0]_s$
T300/934	0.042	16	$[45/-45/0/90]_s$
HMF330C/34	0.054	1	$[(\pm45)/(0/90)]_s$
HMF330C/34	0.108	3	$[(\pm45)/(\mp45)/(0/90)/(90/0)]_s$

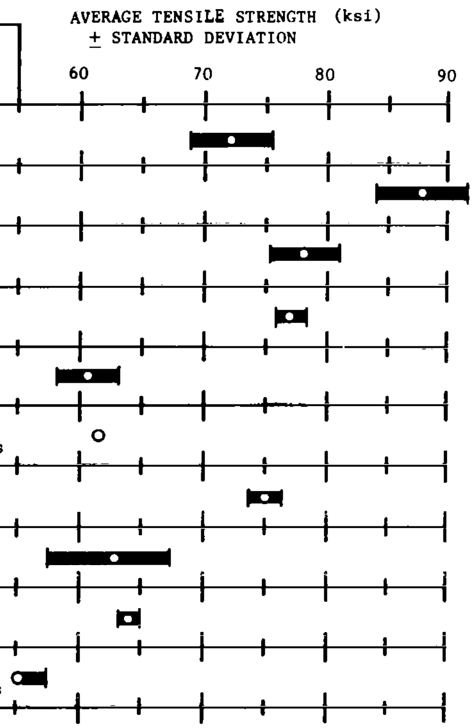

DELAMINATION AND TENSILE STRENGTH

An examination of several independent studies confirms the observation that stacking sequences that are prone to delamination exhibit generally lower ultimate strengths.

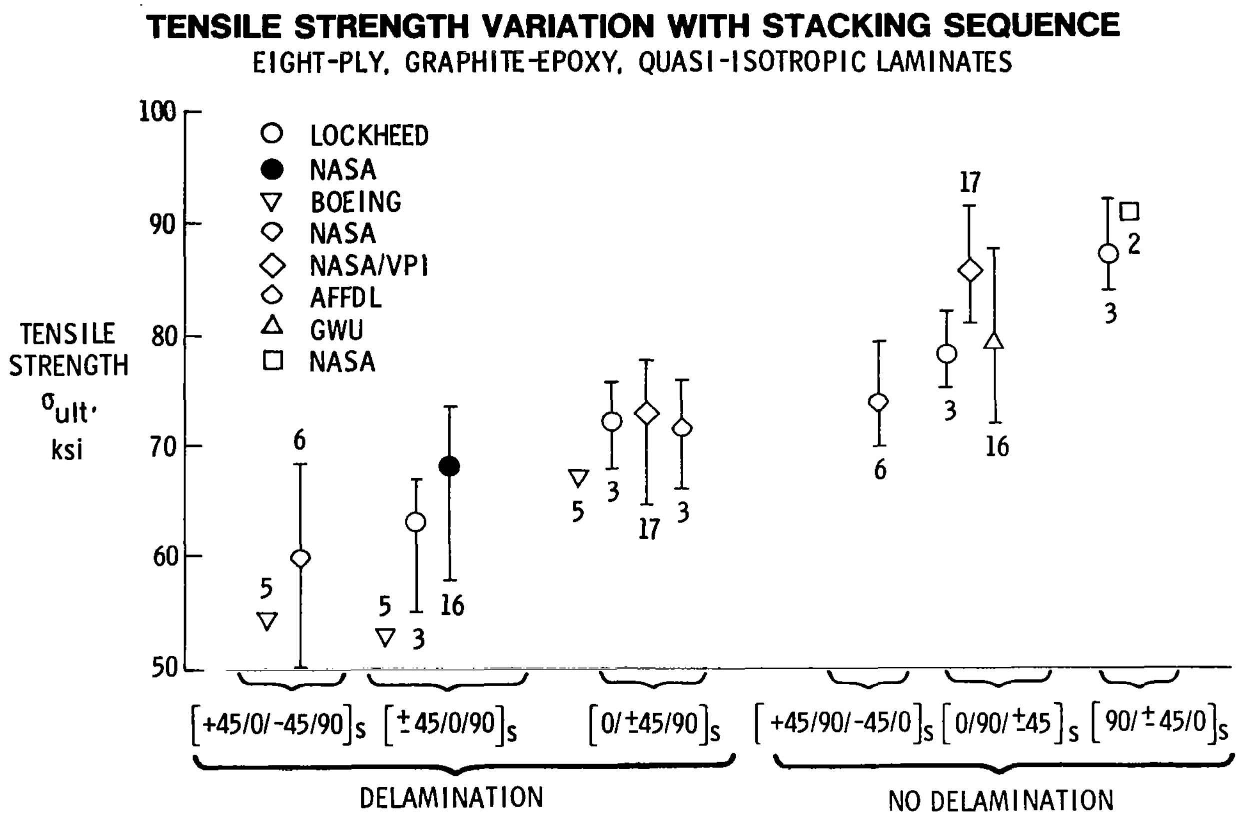

WHAT CAUSES DELAMINATION

Strain gages placed on tensile specimen edges to measure the "through-the-thickness" normal strain (z-strain) as a function of tensile strain (x-strain) showed that the delamination-prone laminates developed a negative Poisson ratio (e.g., the z-strain was positive during tensile loading). Thus interlaminar interaction that was unaccounted for in laminated plate analysis was providing a driving force for delamination.

THROUGH-THICKNESS NORMAL STRAIN ε_Z VERSUS APPLIED TENSILE STRAIN ε_X AS A FUNCTION OF T300/934 PANEL TYPE DESCRIBED IN PREVIOUS FIGURE

{From ref. 1}

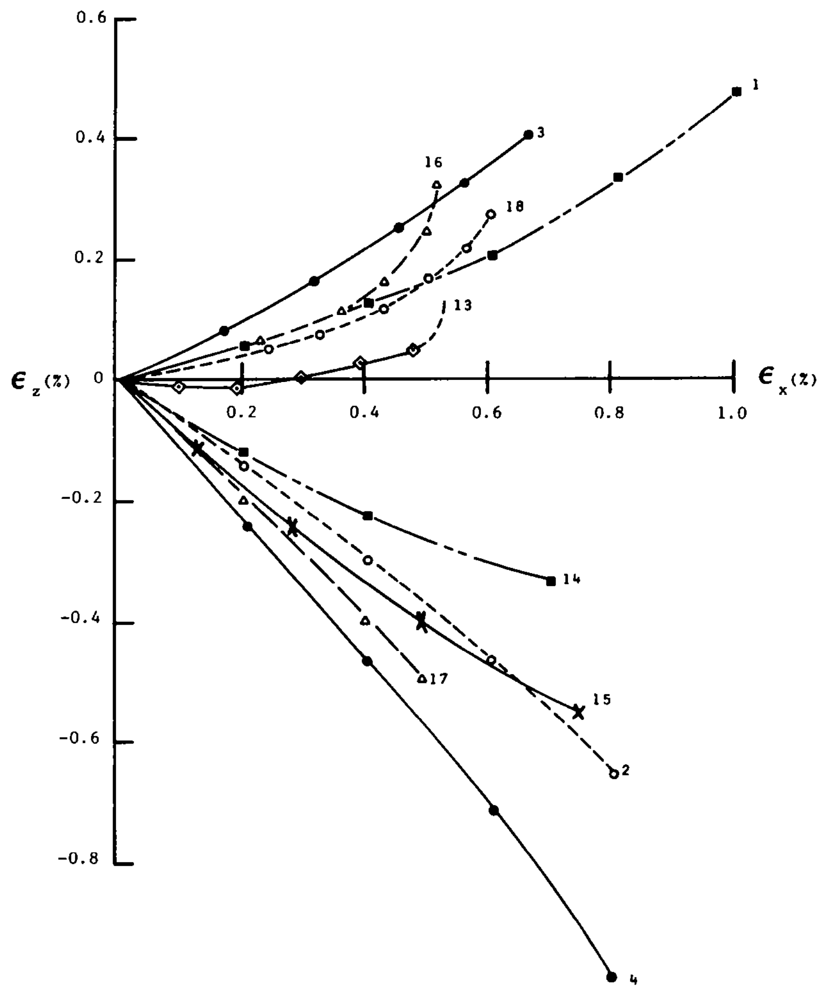

WHERE DOES DELAMINATION OCCUR

Examination of the edges of tensile specimens before and after failure revealed that the location of delamination depended on the particular stacking sequence and in some cases involved multiple delamination at several locations through the ply thickness. Transverse cracks were seen to initiate both before and after delamination, depending on stacking sequence. The extent of delamination was found to be greater at the edges than in the interior of the specimen.

x-z EDGE VIEW OF $(0/45/-45/90)_S$ LAMINATE AFTER LOADING TO 95% UTS
(From ref. 1)

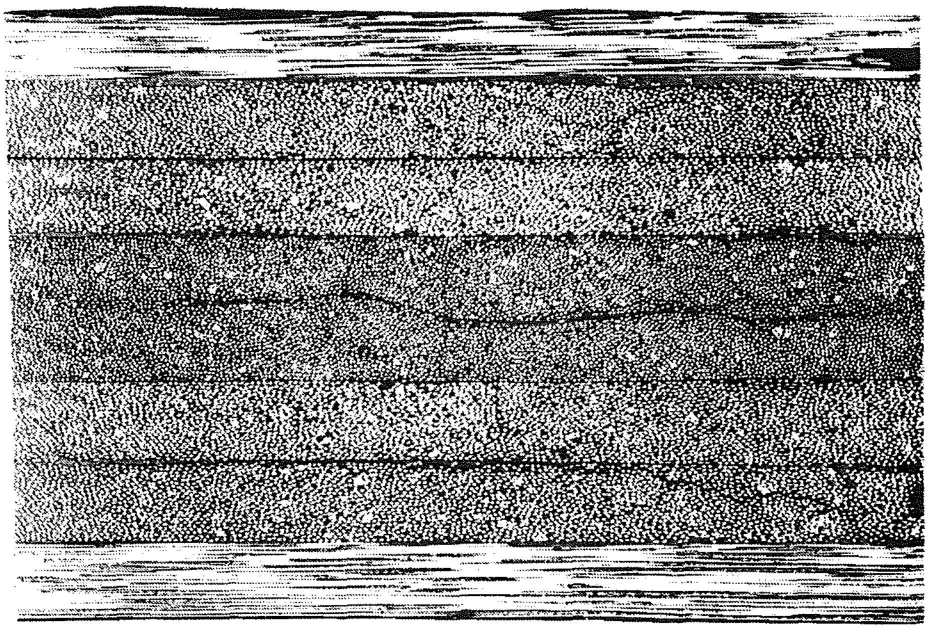

EDGE VIEW OF $(45/-45/0/90)_s$ LAMINATE AFTER LOADING TO 95% UTS

(From ref. 1)

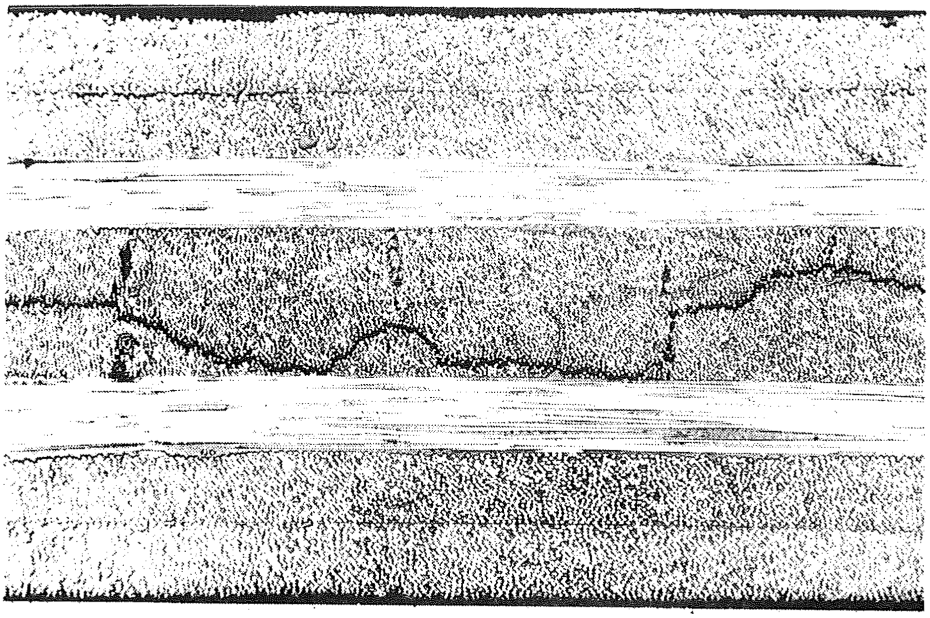

LONGITUDINAL x-z SECTION OF $(45/-45/0/90)_s$ TAKEN NEAR MIDPLANE BY SECTIONING AND POLISHING

(From ref. 1)

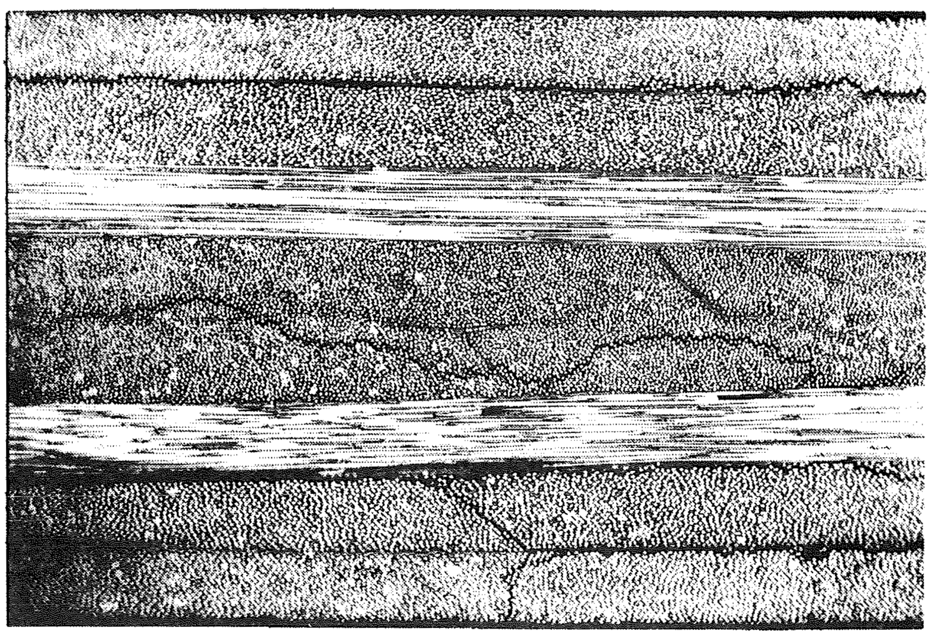

EDGE VIEW OF $(90/45/-45/0)_s$ LAMINATE AFTER LOADING TO 95% UTS
(From ref. 1)

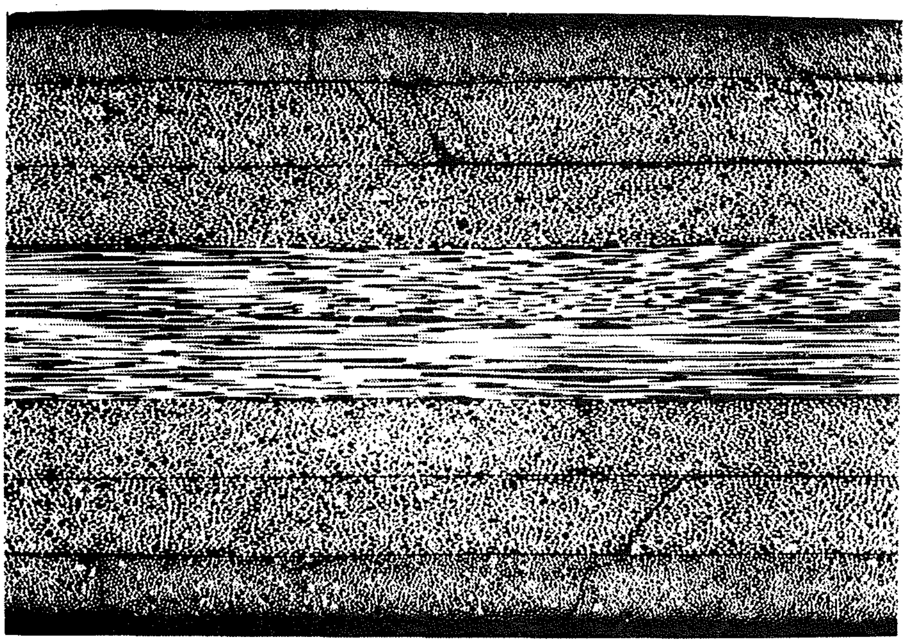

Consideration of stress equilibrium and conservation of angular momentum led to an understanding of how interlaminar stresses arise and the development of simple models to approximate the level and sign of these stresses.

ANISOTROPY IN STIFFNESS OR EXPANSION COEFFICIENTS CAUSES PLY OR LAYER STRESSES

$$\Delta L_c = \frac{V_1 E_1 \Delta L_1 + V_2 E_2 \Delta L_2}{V_1 E_1 + V_2 E_2}$$

$$\sigma_1 = \frac{E_1}{L_0} (\Delta L_c - \Delta L_1)$$

$$\sigma_2 = \frac{E_2}{L_0} (\Delta L_c - \Delta L_2)$$

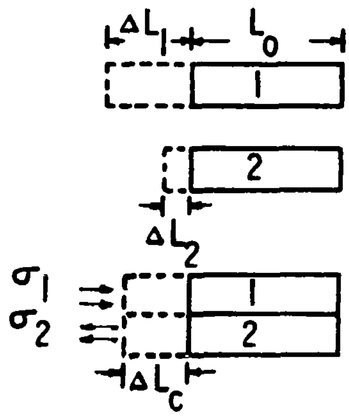

IN-PLANE PLY STRESSES RESULT IN FREE-EDGE STRESSES

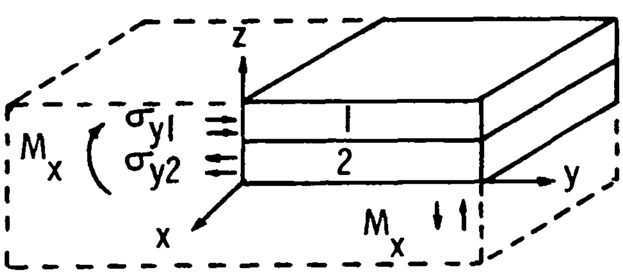

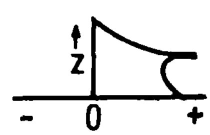

σ_z @ y = b

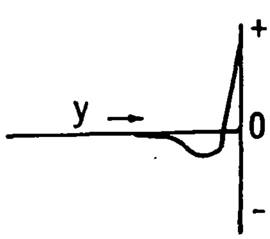

σ_z @ z = 0

NUMERICAL ANALYSIS OF INTERLAMINAR STRESSES

Finite-element and finite-difference analyses have been applied to models of an y-z section of a laminate under uniaxial loading in the x direction. The through-the-thickness Poisson ratio predicted from the analyses agreed well with experimentally measured values.

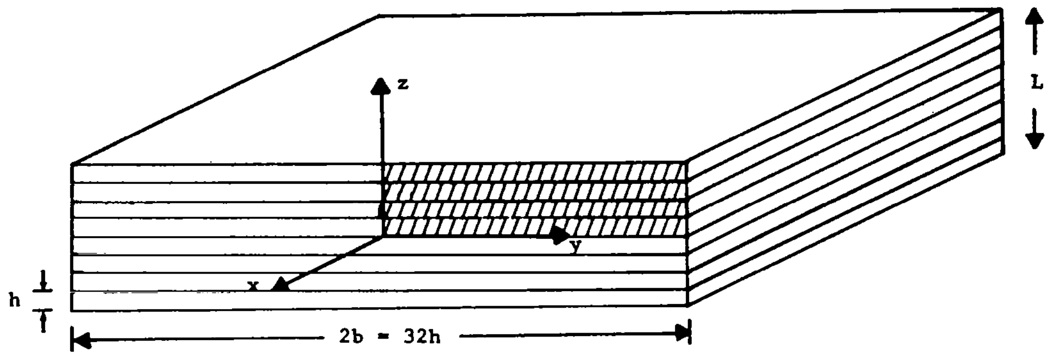

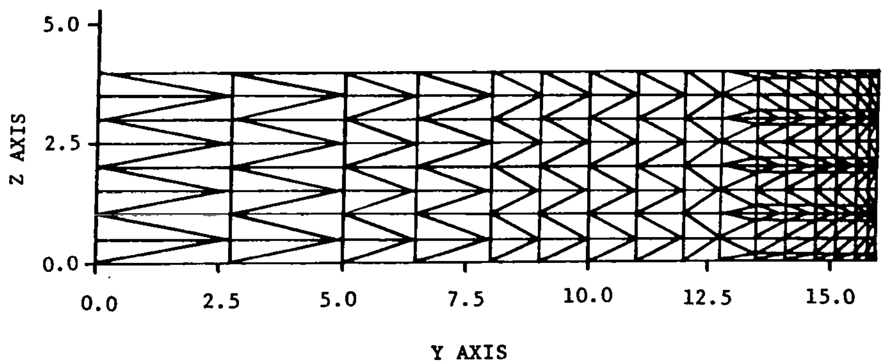

STACKING SEQUENCE DEPENDENCE OF THROUGH THICKNESS CONTRACTION ν_{xz} IN T300/934 QUASI-ISOTROPIC LAMINATES (ref. 1)

Panel No.	Stacking Sequence	ν_{xz} Experimental	ν_{xz} Calculated	Ultimate Tensile Strength (ksi)
15	$[90/45/-45/0]_s$	0.80	0.72	87
13	$[0/45/-45/90]_s$	-0.05	-0.02	72
16	$[45/-45/0/90]_s$	-0.30	-0.34	63

COMPARISON OF NUMERICAL METHODS

The detailed stress analysis was found to depend somewhat on the fineness of the model discretization and the order of the assumed variation of displacement or stress field in the case of finite-element analysis. Stress gradients in both the y and z directions were found in these analyses, as shown in the figures that follow.

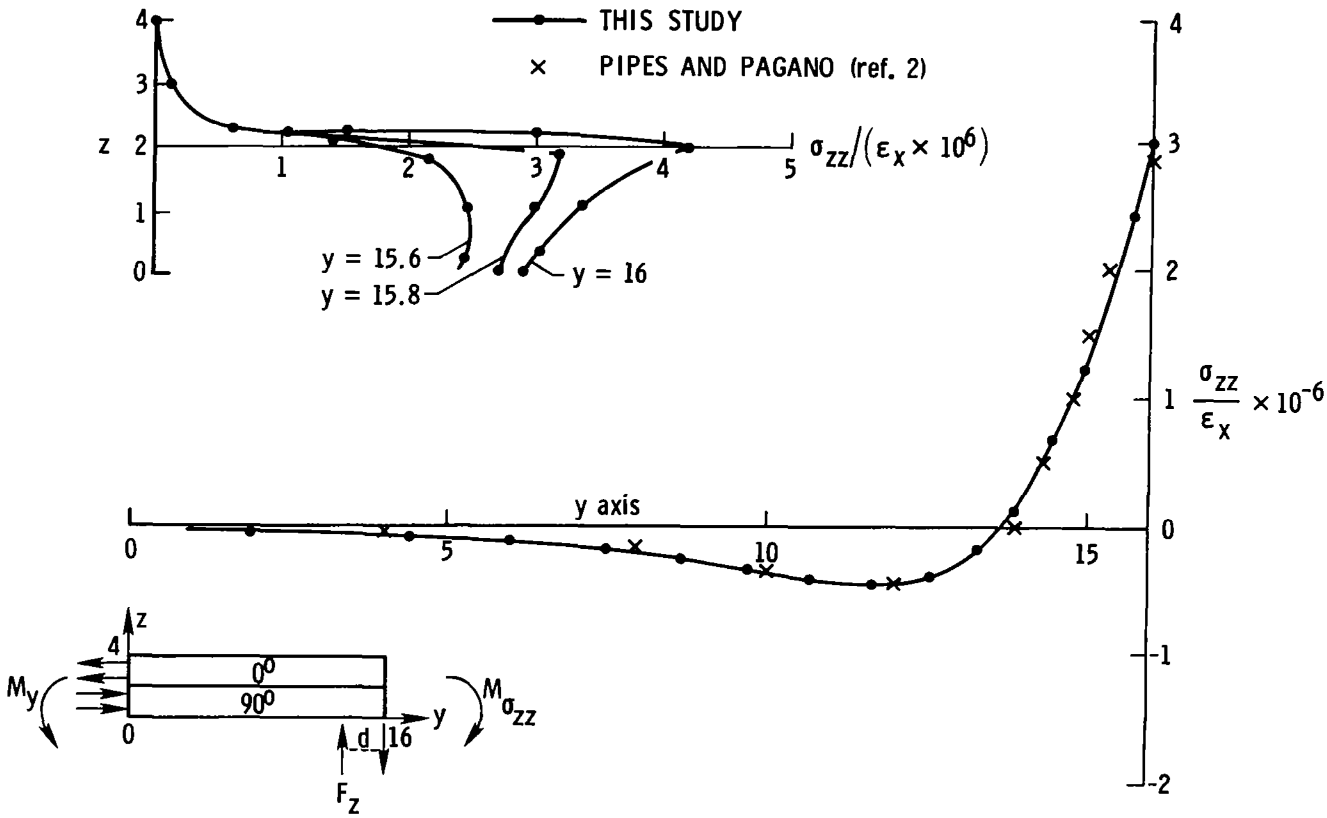

FREE EDGE STRESSES IN $[0, 90, 90, 0]_T$ T300/934

THROUGH-THICKNESS DISTRIBUTION OF σ_2 NEAR FREE EDGE

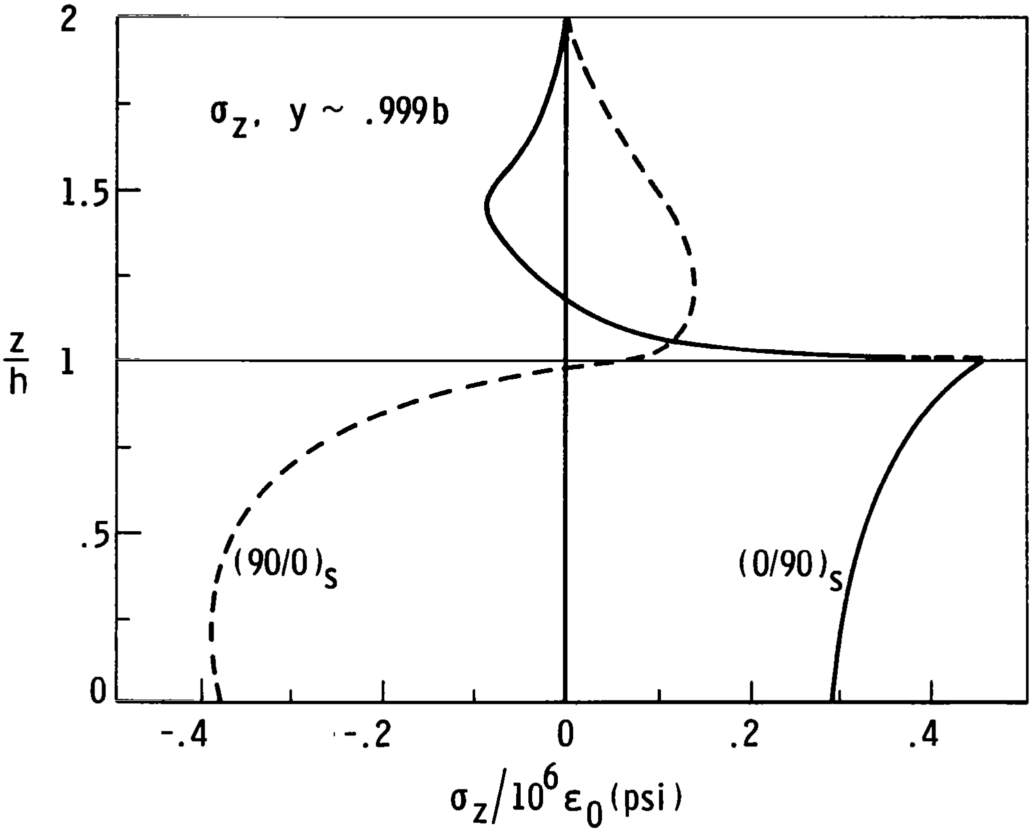

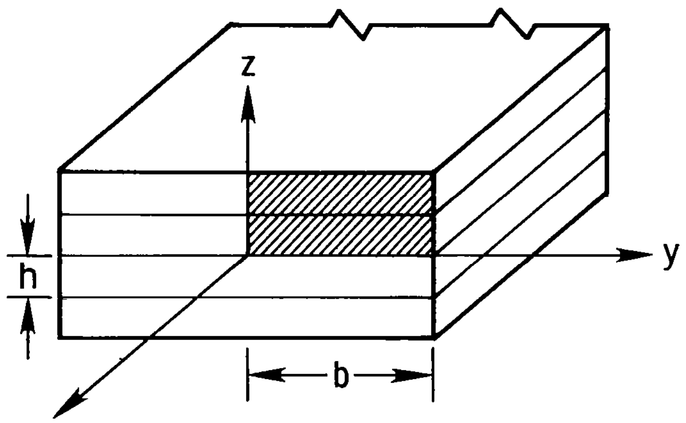

PREDICTION OF DELAMINATION LOCATION

As shown in the figures, the location of peak tensile stress in the analysis often agreed with the experimentally observed delamination location.

DISTRIBUTION OF σ_Z NEAR FREE EDGE UNDER TENSILE LOAD IN x DIRECTION

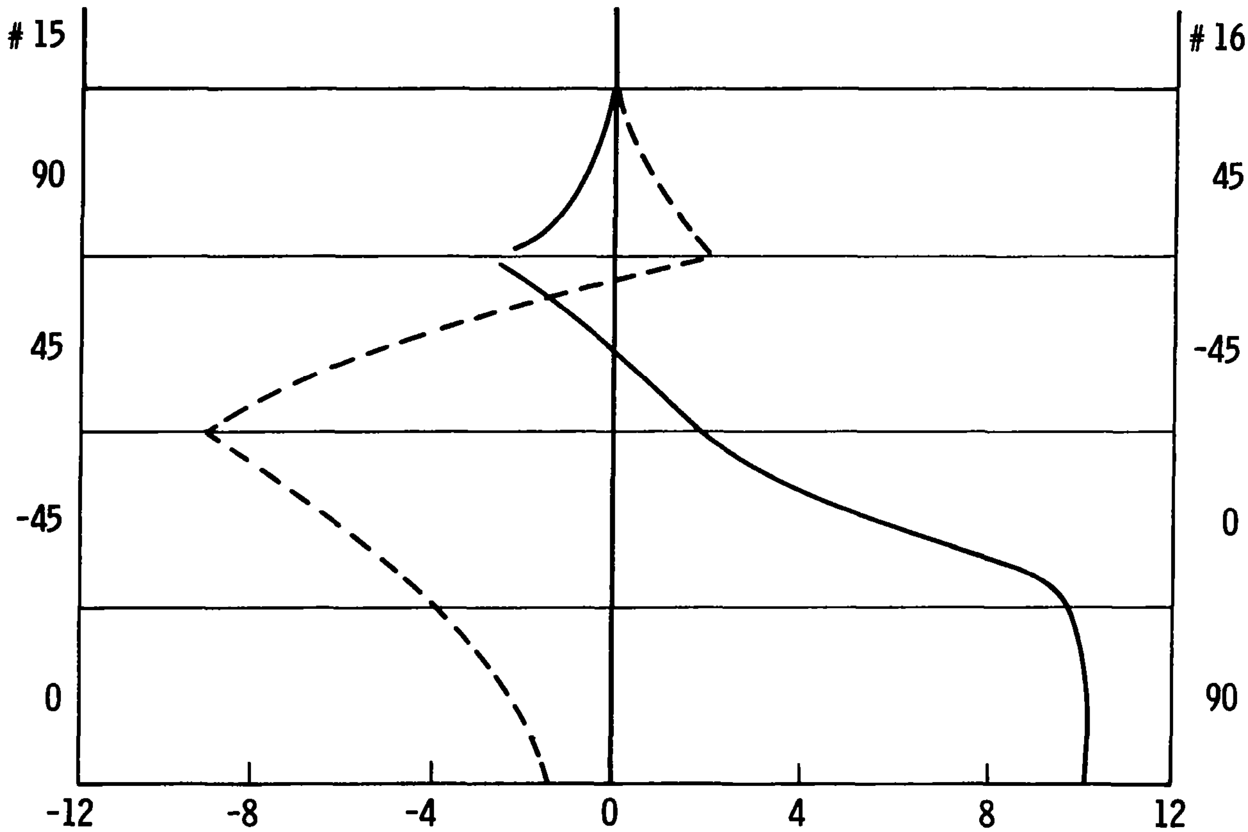

σ_Z, y = .999b

ε_X = .4%

LONGITUDINAL x-z PLANE SECTION AT FREE EDGE OF $(90/\pm45/0)_s$ SPECIMEN
(From ref. 1)

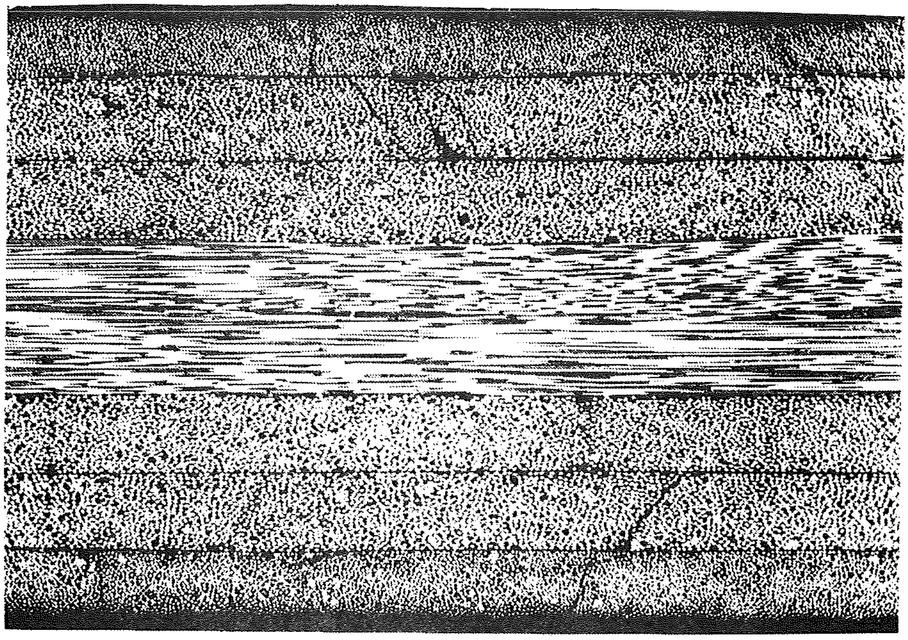

LONGITUDINAL x-z PLANE SECTION NEAR CENTER LINE OF $(\pm45/0/90)_s$ SPECIMEN
(From ref. 1)

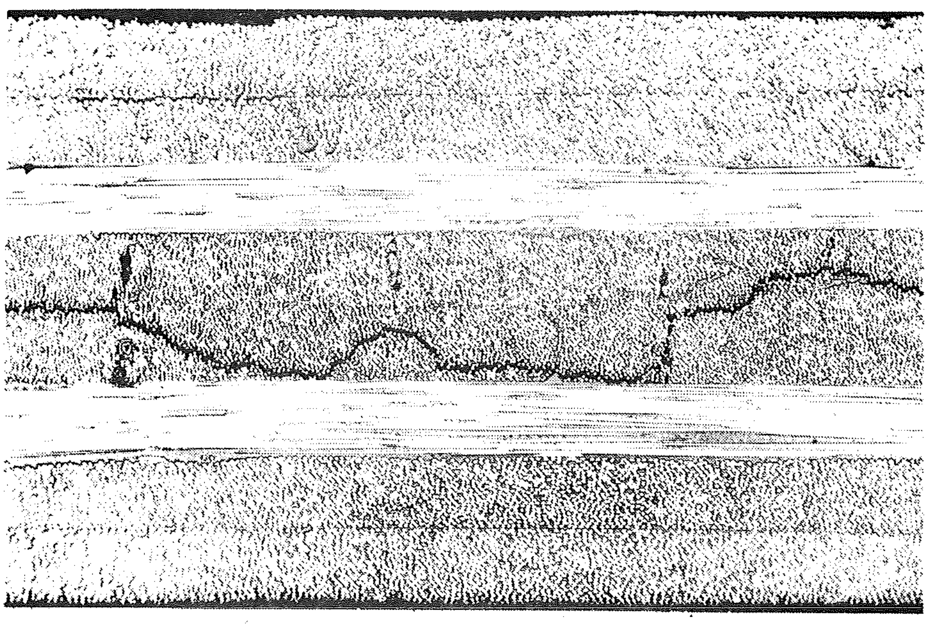

A problem arose, however, when the numerical analysis of interlaminar stresses associated with moisture gradients was considered. The figures show the moisture concentration as a function of y,z position at two different times during the moisture absorption process. At a time that was small with respect to the equilibrium time, the gradient of concentration is very steep near the free edge. In the limit of very small times, this gradient is infinitely steep. Since absorbed moisture is known to swell the composite locally, a gradient of hygroscopically induced stresses is introduced.

AVERAGE WEIGHT GAIN (LOSS) DURING ABSORPTION (DESORPTION) RELATIVE TO EQUILIBRIUM MOISTURE CONTENT M_s

{From ref. 3}

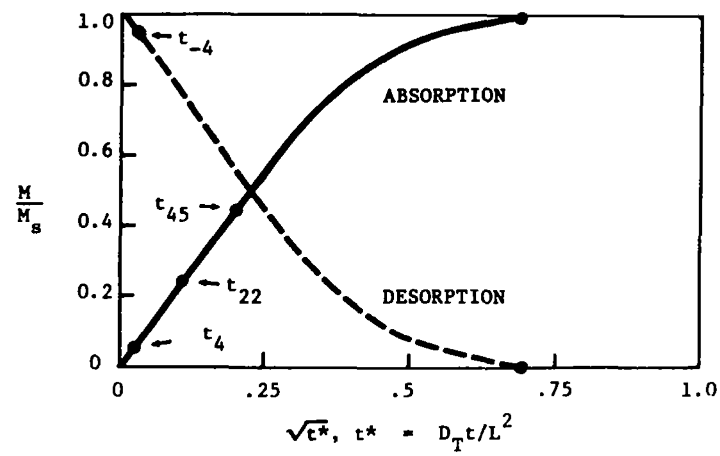

MOISTURE CONCENTRATION C/C_S AFTER ABSORPTION TIME t_4 ($M/M_S \approx 4\%$)

{From ref. 3}

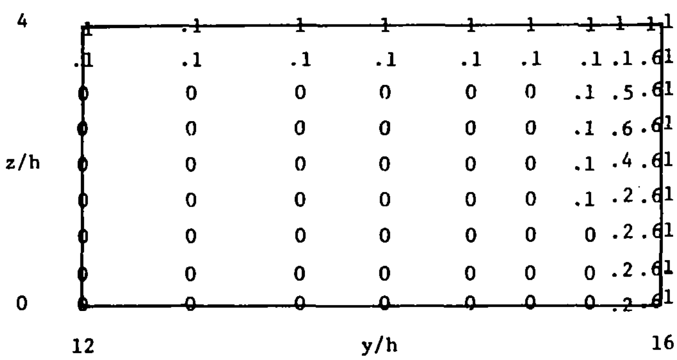

MOISTURE CONCENTRATION C/C_S AFTER ABSORPTION TIME t_{45}
($M/M_S \approx 45\%$)

{From ref. 3}

4	1	1	1	1	1	1	1	1	1	1
	.9	.9	.9	.9	.9	.1	1	1	1	1
	.7	.8	.8	.8	.9	.9	1	1	1	1
	.6	.7	.7	.8	.8	.9	.9	1	1	1
z/h	.5	.6	.6	.7	.8	.8	.9	1	1	1
	.4	.5	.6	.6	.7	.8	.9	.9	1	1
	.3	.4	.5	.6	.7	.8	.9	.9	1	1
	.3	.3	.4	.5	.7	.8	.9	.9	1	1
0	.2	.3	.4	.5	.7	.8	.9	.9	1	1
	12			y/h						16

PREDICTION OF DELAMINATION UNDER A STRESS GRADIENT

The results of stress analysis in a unidirectional laminate during desorption of moisture from an initially saturated condition show that a transverse normal stress greater than the transverse tensile strength of the material is present during the first part of the desorption period, but gradually reduces to zero upon drying out. Although strength theories based on these local stresses predict delamination during desorption, no experimental evidence of delamination was found in a series of experiments conducted under a NASA Ames contract (ref. 3). It was recognized during the analysis of these results that stresses calculated at a distance from the free edge or interlaminar region which is on the order of the fiber diameter cannot be physically real. The analysis is based on the assumption that fiber and matrix phases are smeared together at the lamina level. That assumption is not appropriate on the microstructural scale. At this level, the interaction of individual fibers and intervening matrix must be considered. Thus the analysis of interlaminar stresses is inherently limited to a cross-sectional area which contains on the order of 10 fibers. In graphite-epoxy laminates this results in a minimum finite-element size of approximately 0.001 × 0.001 in.

σ_z THROUGH-THICKNESS DISTRIBUTION NEAR FREE EDGE OF UNIDIRECTIONAL 8-PLY LAMINATE DURING DESORPTION FROM EQUILIBRIUM MOISTURE CONTENT M_S

{From ref. 3}

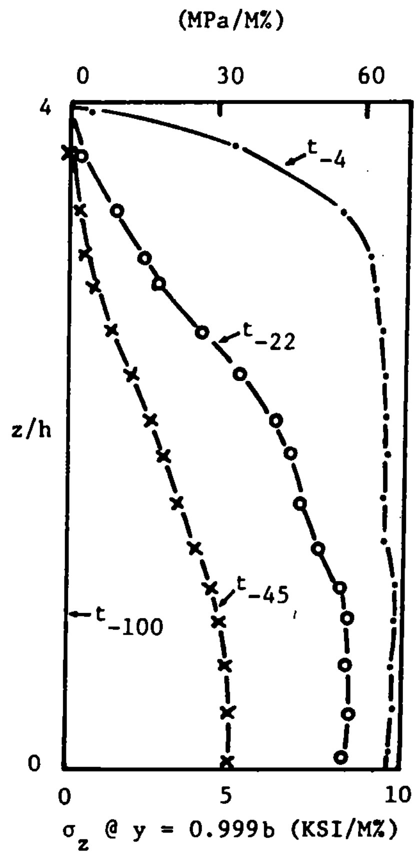

5-8

σ_Z DISTRIBUTION ALONG MIDPLANE OF UNIDIRECTIONAL 8-PLY LAMINATE DURING DESORPTION

{From ref. 3}

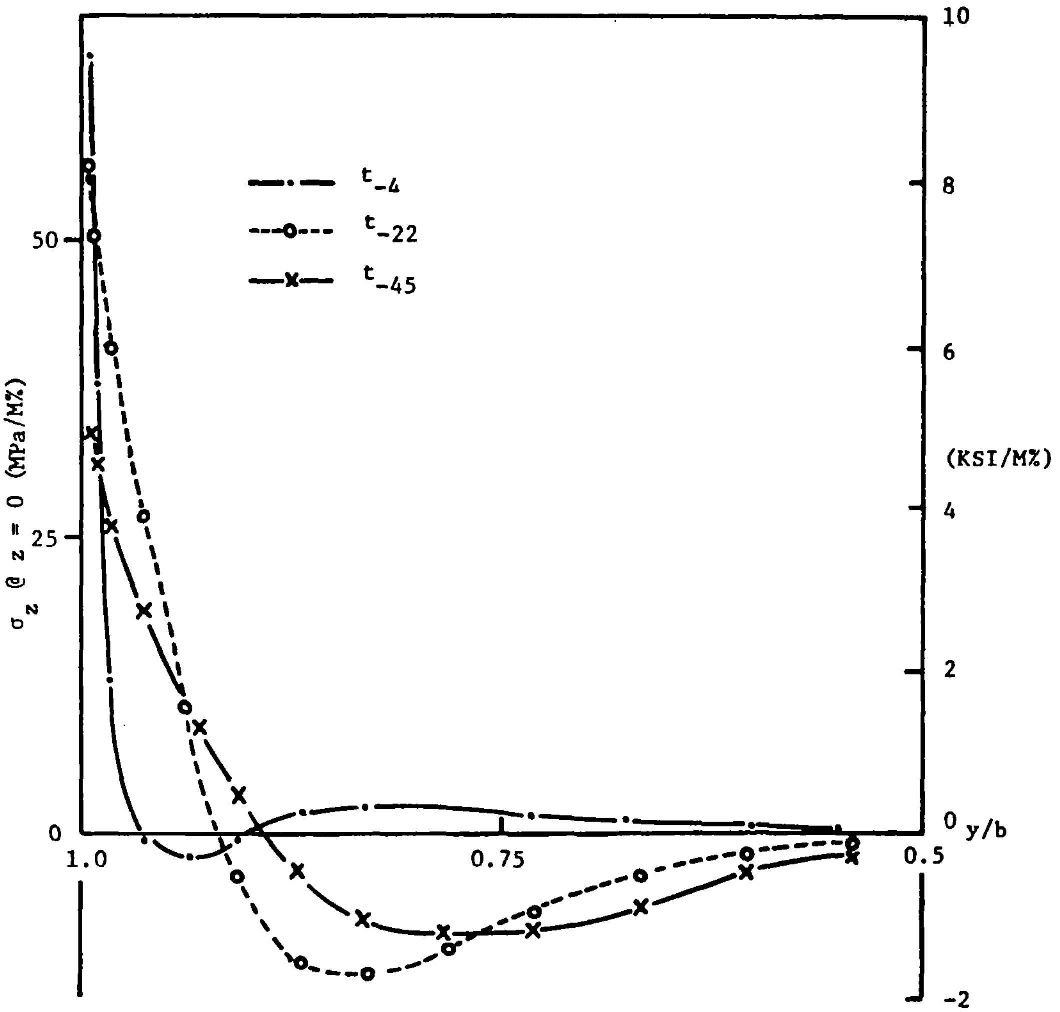

PLY THICKNESS AFFECTS DELAMINATION ONSET STRESS

Rodini and Eisenmann (ref. 4) found that the onset stress in a series of quasi-isotropic laminates varied with ply thickness as approximately 1 over the square root of laminate thickness. Delamination stress analysis based on continuum theory is independent of the scale of the structure and was unable to predict the experimental results. Rodini et al. proposed that Weibull strength theory which is dependent on specimen volume could be used to explain the results.

A second approach, based on fracture mechanics, was taken at Drexel and Lockheed to account for the observed size dependence of delamination and transverse cracking onset in a series of tensile-loaded (25/-25/90n)s laminates where n ranged from 1/2 to 8 (ref. 5).

PLY THICKNESS EFFECTS

T300/5208 LAMINATES	AT ONSET OF DELAMINATION	
	EXPERIMENT	PREDICTION
$(\pm 45/0/90)_s$	45.3 ksi	
	45.3	49.0 ksi
	45.5	
$(\pm 45_2/0_2/90_2)_s$	38.3	
	38.6	36.0
	37.8	
$(\pm 45_3/0_3/90_3)_s$	28.7	
	30.7	29.0

CASE STUDY USING T300/934 GRAPHITE-EPOXY LAMINATES

Laminate configuration:

$(\pm 25/90_n)_s$ $n = \frac{1}{2}, 1, 2, 3, 4, 6, 8$

Loading condition:

Uniaxial laminate tension $\bar{\sigma}_x$ or $\bar{\varepsilon}_x$

Uniform curing temperature $\Delta T = T_o - T_{r,t}$

Types of cracking studied:

1. Transverse cracks in 90^o layer
2. Edge delamination along 90/90 interface (mode I) and 25/90 interface (mixed mode), and transverse-crack-induced delamination
3. Edge-delamination-induced transverse cracks

Objectives of study:

1. Onset and growth behavior of various modes of damage
2. Their interrelations
3. Physical and/or geometrical parameters influencing these behaviors
4. Whether minimechanics approach is viable tool in studying damages in composite laminates
5. How to bridge gap between micromechanics and macromechanics

SCHEMATIC OF FRACTURE SEQUENCE IN $(25/-25/90_n)_S$ LAMINATES (ref. 5)

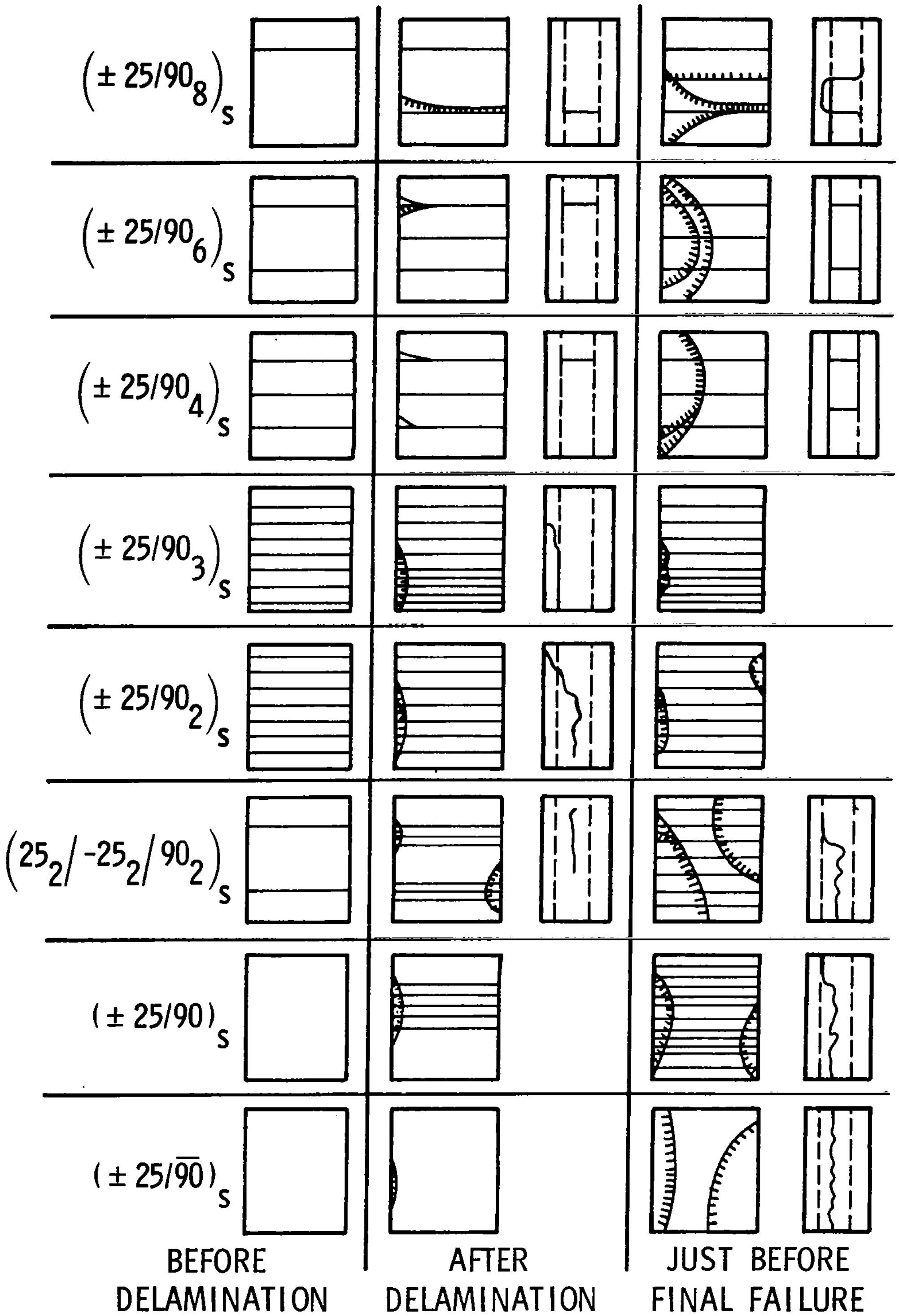

OBSERVED TENSILE STRAIN E_X FOR TRANSVERSE CRACKING, DELAMINATION, AND ULTIMATE FAILURE VERSUS NUMBER OF 90° PLIES IN T300/934

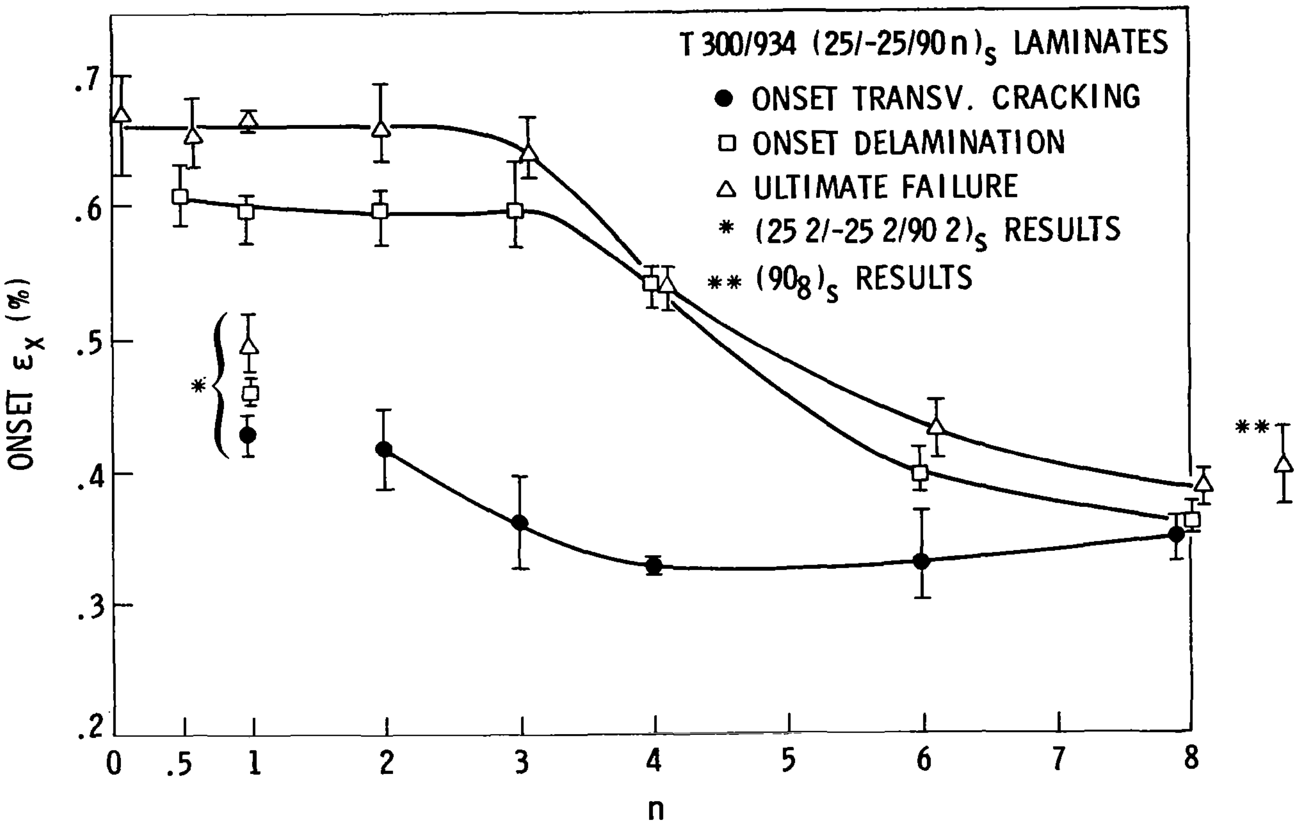

ANALYSIS OF DELAMINATION STRAIN ENERGY RELEASE BY CRACK CLOSURE

The crack closure method pioneered for delamination analysis by Rybicki et al. (ref. 6) was applied to the analysis of strain energy release rate associated with both delamination and transverse cracking. The analysis accounted for the contribution of thermal stresses to the total energy release rate. The crack closure method also allows the determination of the G values associated with each crack opening mode.

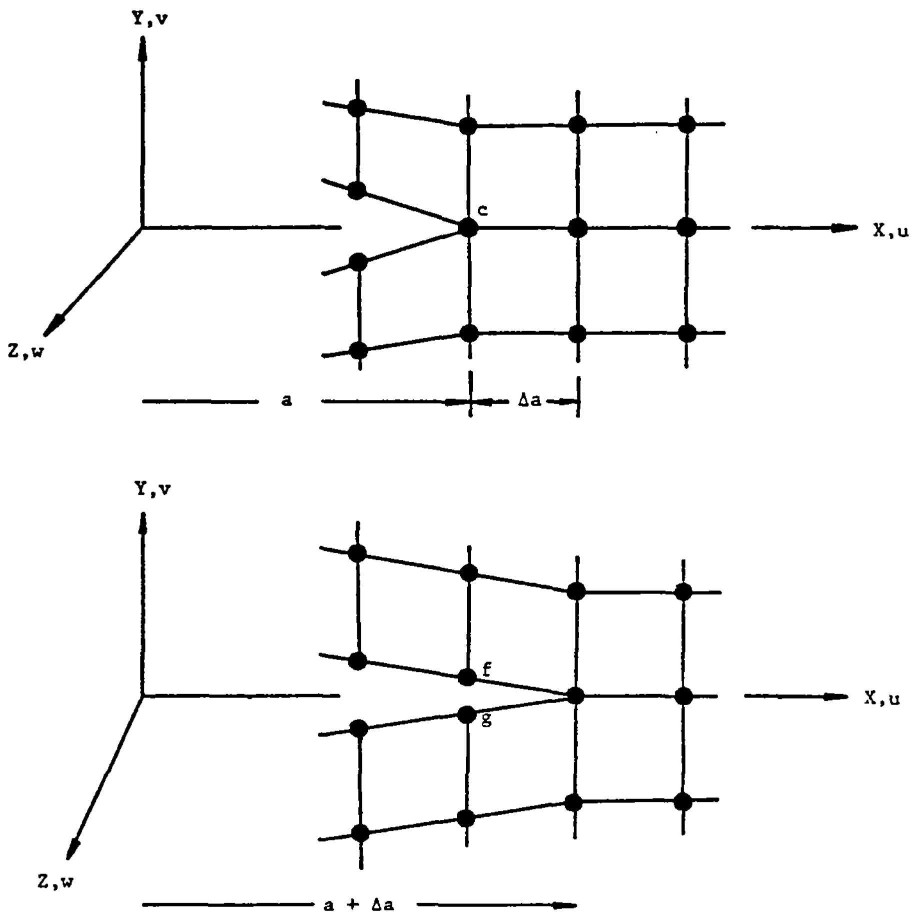

The work required to close the crack extension is approximated by

$$\Delta W \sim [F_x(u_f-u_g) + F_y(v_f-v_g) + F_z(w_f-w_g)]/2$$

where F_x, F_y, F_z are the components of the nodal forces required to close nodes f and g together. Thus, the energy release rates for the three crack extension modes are approximated by:

$$G_I \sim F_y(v_f-v_g)/2\Delta a$$

$$G_{II} \sim F_x(u_f-u_g)/2\Delta a$$

$$G_{III} \sim F_z(w_f-w_g)/2\Delta a$$

ENERGY ANALYSIS

$$G = -\frac{du}{da} \approx -\frac{\Delta u}{\Delta a}$$

Energy released in crack opening equals work required to close crack:

$$-\Delta u = \tfrac{1}{2}\tilde{F} \cdot \tilde{D}$$

Let $\tilde{F}_e$, $\tilde{D}_e$ be the elastic solution for a loading of $\varepsilon_x = 10^{-6}$ and let $\tilde{F}_T$, $\tilde{D}_T$ be the elastic solution for a loading of $\Delta T = -1^oF$.

Then

$$G = \frac{1}{2\Delta a} \{\tilde{F}_e(\varepsilon_x) + \tilde{F}_T(\Delta T)\} \cdot \{\tilde{D}_e(\varepsilon_x) + \tilde{D}_T(\Delta T)\}$$

This may be rewritten as

$$G = t\{C_e(\varepsilon_x)^2 + C_{eT}(\varepsilon_x)(\Delta T) + C_T(\Delta T)^2\}$$

THE CRITICAL FLAW CONCEPT

The next figure below introduces the concept of an effective flaw which preexists in a material prior to loading or one which grows subcritically in the sense of satisfying the Griffith critical stress criterion based on independently measured stiffness and toughness.

If a critical flaw is not assumed to exist, then the analysis of transverse cracking of progressively thicker 90° layers in the (25/-25/90n)s laminate predicts that the energy release rate goes to infinity as the ply thickness is increased without limit. The consequence of this is that the predicted stress level for transverse cracking approaches zero for very thick 90° layers. This is inconsistent with the finite strength of transversely loaded unidirectional composites.

METHOD OF LINEAR FRACTURE MECHANICS

- CONCEPT OF ENERGY RELEASE RATE
- G-CURVES AS FUNCTIONS OF CRACK EXTENSION

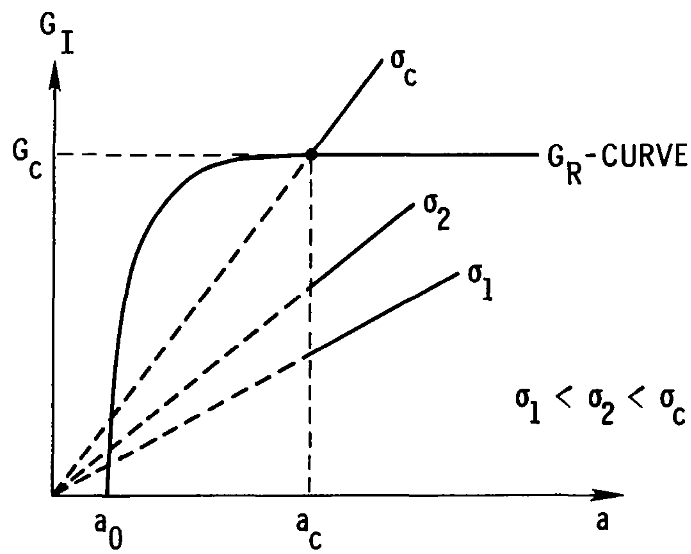

FOR MODE-I COLLINEAR CRACKING IN ISOTROPIC ELASTIC SOLIDS,

$$G_I = (\pi/E)\, a\sigma^2$$

CRITERION FOR CRACK GROWTH:

$$G_I \Big|_{a_c} \rightarrow G_c$$

HENCE

$$\sigma_c = \sqrt{(G_c E)/(\pi a_c)}$$

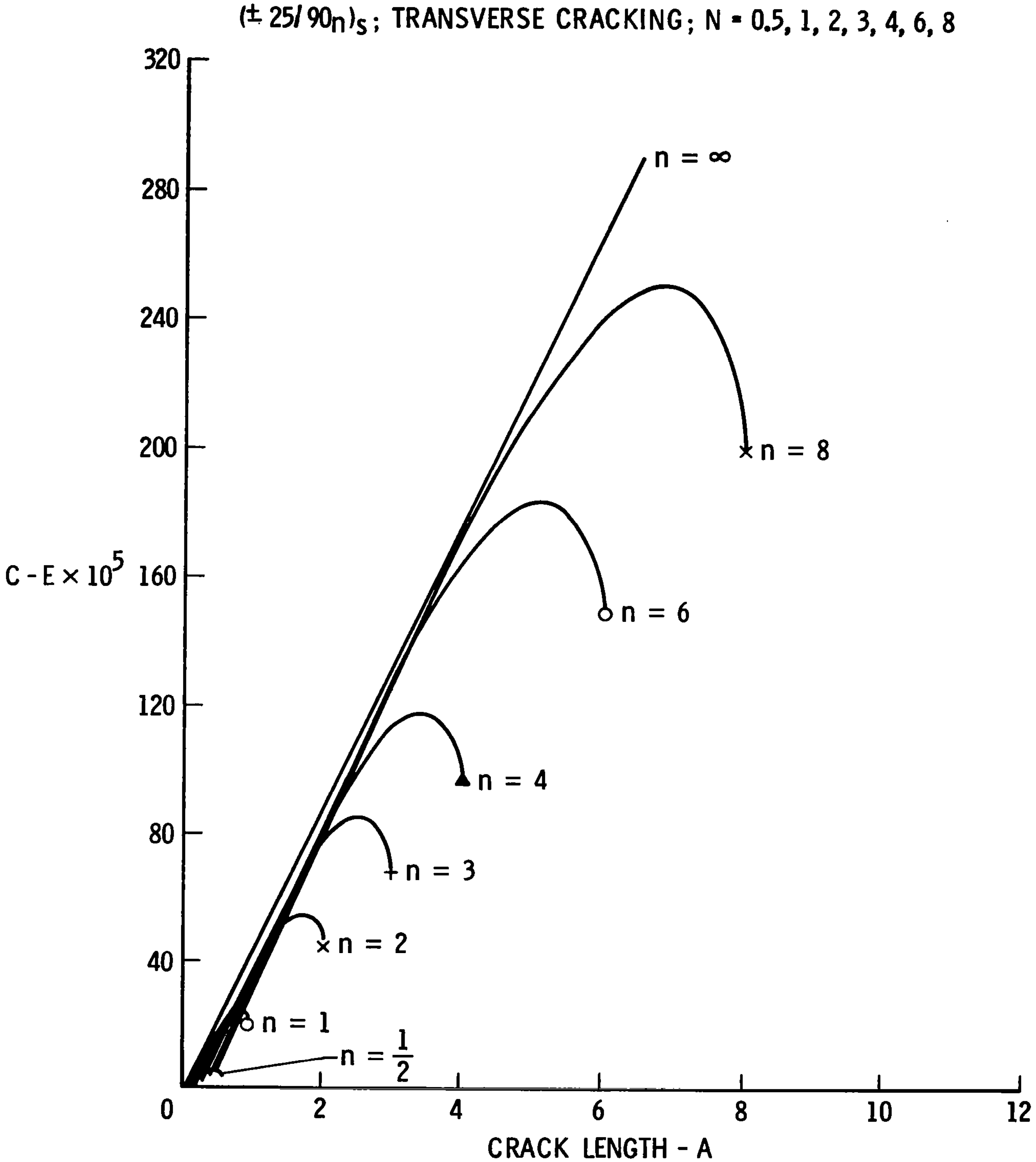

(± 25/90n)s; TRANSVERSE CRACKING; N = 0.5, 1, 2, 3, 4, 6, 8
C - E × 10^5
320
280
240
200
160
120
80
40
0
2
4
6
8
10
12
CRACK LENGTH - A
n = ∞
n = 8
n = 6
n = 4
n = 3
n = 2
n = 1
n = 1/2

DETERMINATION OF THE CRITICAL FLAW SIZE

To determine the critical flaw size a_c, we postulate that it can be calculated by knowledge of the independently measured elastic modulus E the fracture toughness G_{Ic} and the unnotched tensile strength in the longitudinal and transverse directions. For T300/934 composites, the substitution of these quantities into the Griffith equation

$$a_c = \left(\frac{EG_{Ic}}{\pi}\right) \Big/ \sigma^2$$

gives a_c(transverse) = 0.010 in. and a_c(longitudinal) = 0.020 in. Since these are both much larger than the fiber diameter, our assumption of homogeneous ply properties in deriving the effective flaw size is consistent with the absolute size of the flaw. The transverse critical flaw size was applied to the analysis of transverse and delamination crack initiation in the analysis. The relative sizes of a_c and a_m are important in assessing the stability of delamination growth, which is found to depend on the 90° ply thickness in the (25/-25/90n)s experiments.

BEHAVIOR OF G-CURVES IN FREE-EDGE DELAMINATION

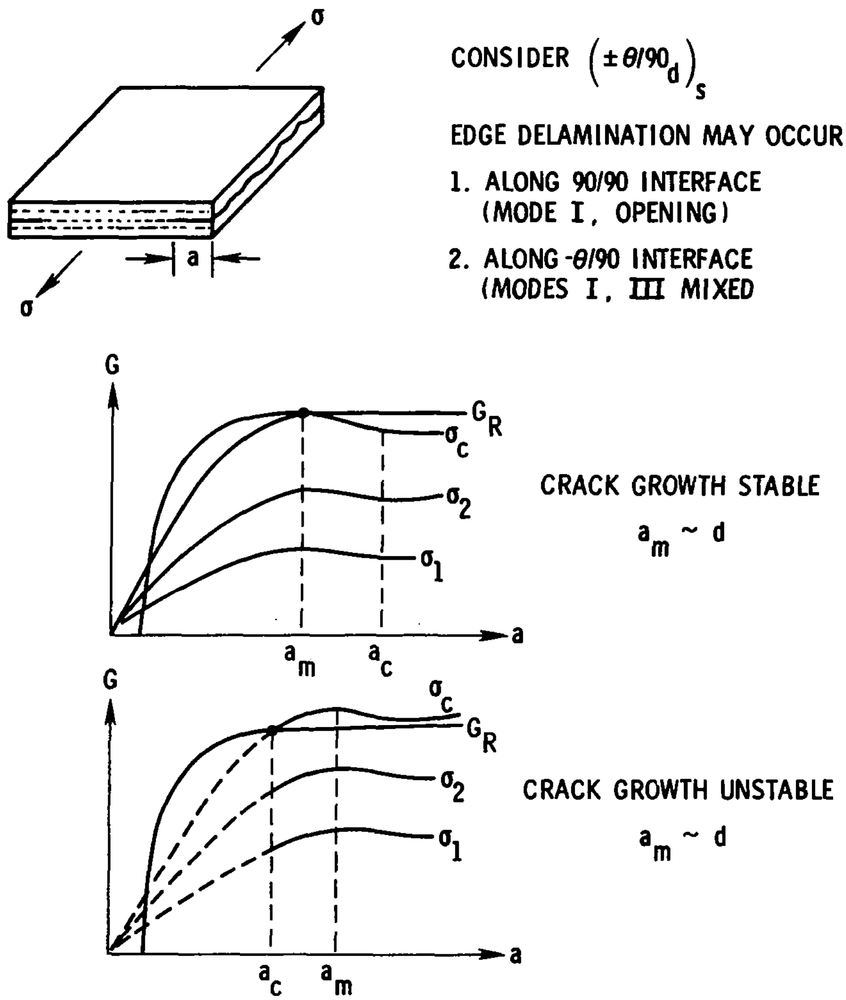

Energy release rate analysis is qualitatively and quantitatively successful in predicting experimental behavior.

OBSERVED TENSILE STRAIN E_X FOR TRANSVERSE CRACKING, DELAMINATION, AND ULTIMATE FAILURE VERSUS NUMBER OF 90° PLIES IN T300/934

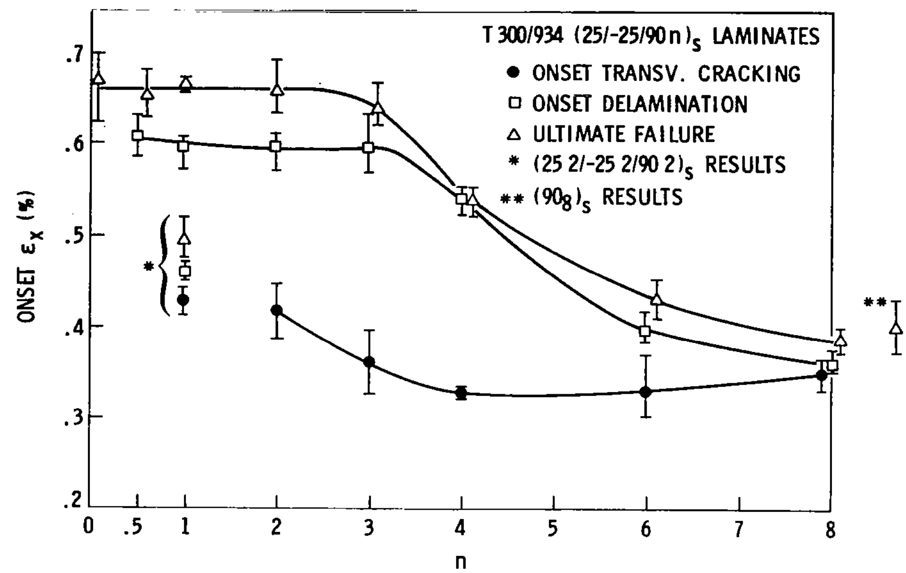

COMPARISON BETWEEN THEORY (DOTTED LINES) AND EXPERIMENT (PREDICTION BASED ON G_C = 1.4; a_C = 0.008" AND ΔT = 225°F)

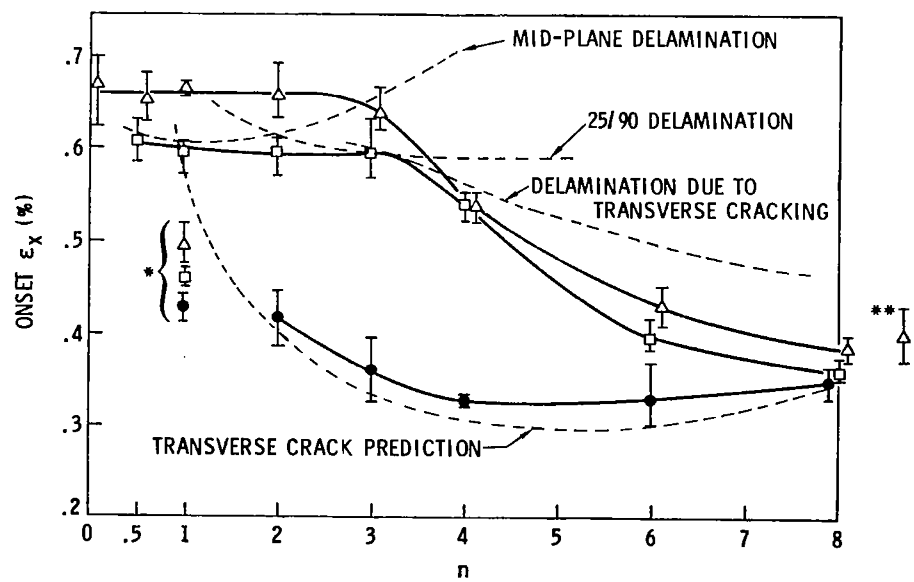

IMPROVING THE RESISTANCE TO DELAMINATION

From the fracture mechanics analysis of delamination onset, it is clear that the onset stress for delamination can be raised if the critical energy release rate (or delamination toughness) of the material can be improved. The table given below shows (1) that order-of-magnitude improvements in matrix toughness do not translate into large improvements in the composite prepregged from tape, and (2) that composites fabricated from cloth prepreg show greater improvement in toughness than do the tape materials. The references presented emphasize the importance of microstructural factors in controlling (and limiting) improvements in delamination toughness.

FRACTURE ENERGIES OF GRAPHITE-EPOXY MATRIX COMPOSITES

Material	Ref.	Resin or Interlaminar Fracture Energy (K J/m^2)	Comments
5208	7	0.076	TGMA / DDS Matrix
Code 69/HTS Graphite Tape	8	0.076	"
5206/Morg II Graphite Tape	9	0.17	"
F263/T200 Graphite Cloth	7	0.36	"
5206/Morg II Tape			
UD Cross Fiber	9	20.4	
$(\pm 45)_s$ Cross Fiber	9	7.8	
QI Cross Fiber	9	9.6	
A	10	0.16	MY750 / NMA / BDMA
A/HMS Tape	10	0.24	
B	10	0.33	MY750 / Piperidine
B/HMS Tape	10	0.28	
C	10	1.40	MY750 / 3.2% CTBN
C/HMS Tape	10	0.37	
D	10	2.2	MY750 / 6.2% CTBN
D/HMS Tape	10	0.36	
E	10	3.20	MY750 / 9% CTBN
E/HMS Tape	10	0.49	
205	7	0.27	Diglycidyl ether bisphenol A/
205/T300 Graphite Cloth	7	0.60	Novalac/Dicyandiamine Catalyst
205+CTBN	7	5.1	13x12 3000 tow T300 cloth
205+CTBN/T300 Graphite Cloth	7	4.6	CTBN + HYCAR additives

STIFFNESS/STRENGTH RELATIONSHIPS

A current Lockheed/NASA study is emphasizing the development of a structural analysis approach to assess the influence of transverse cracking and delamination on the resulting laminate stiffness and strength properties.

OBJECTIVE

- DEVELOP " STRUCTURAL" ANALYSIS FOR LAMINATES WITH ARBITRARY LAYUPS
- PREDICT RELATIONSHIP OF MATRIX CRACKING AND DELAMINATION TO LAMINATE STIFFNESS AND TENSILE STRENGTH

PREMISE

- A LAMINATE IS A STRUCTURE
- MATRIX CRACKS AND DELAMINATIONS MAY OR MAY NOT BE DAMAGE
- A "STRUCTURAL" ANALYSIS OF ARBITRARY LAYUPS IS NEEDED

SHEAR STIFFNESS REDUCTION

Finite-element analysis was used to determine the effective in-plane transverse and shear moduli as a function of transverse crack density. The results indicate that for the experimentally determined crack densities, the loss of in-plane stiffness due to transverse cracking is very small.

SHEAR STIFFNESS REDUCTION AS A FUNCTION OF CRACK SPACING

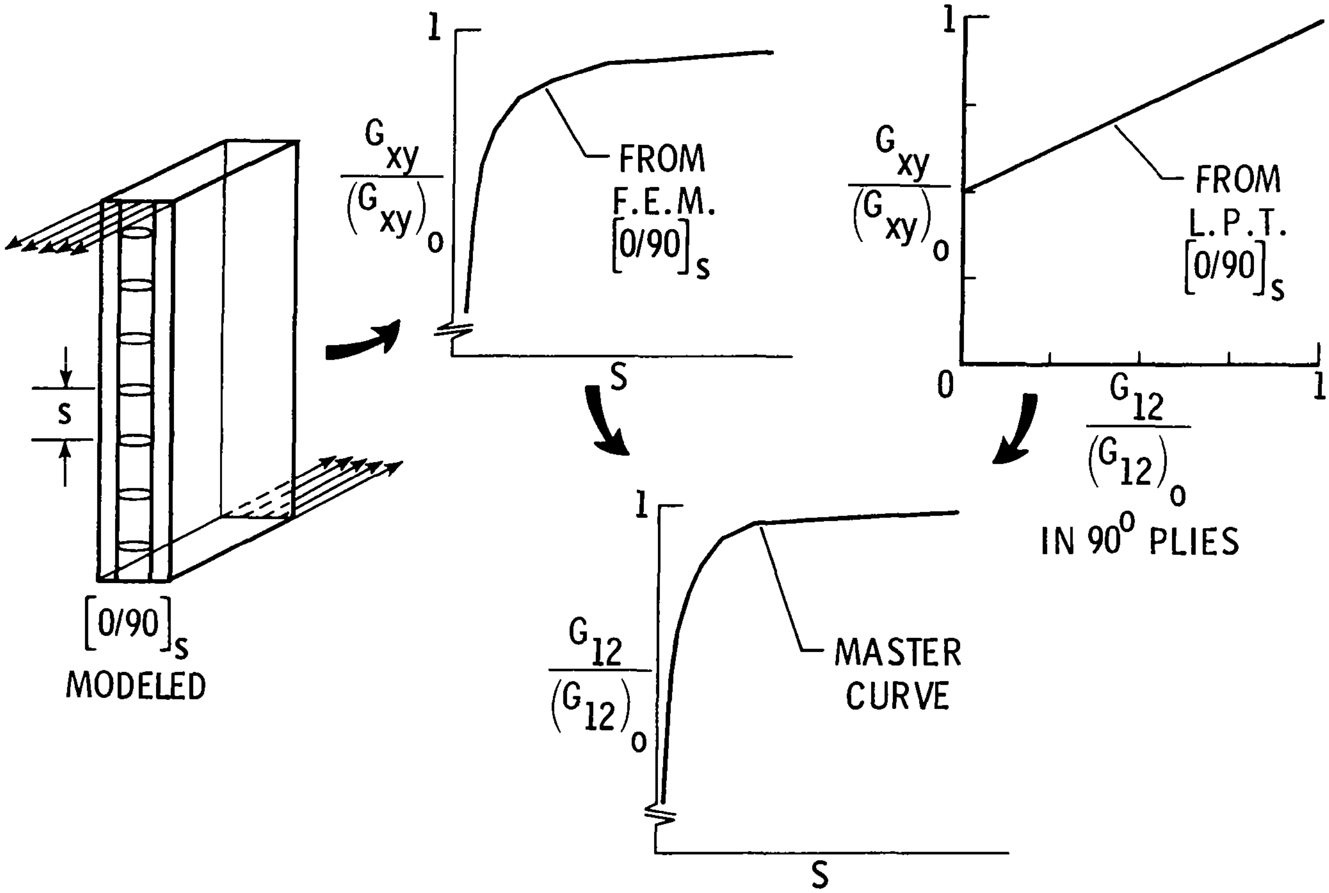

LAMINA STIFFNESS LOSS AS A FUNCTION OF CRACK SPACING

MASTER CURVES

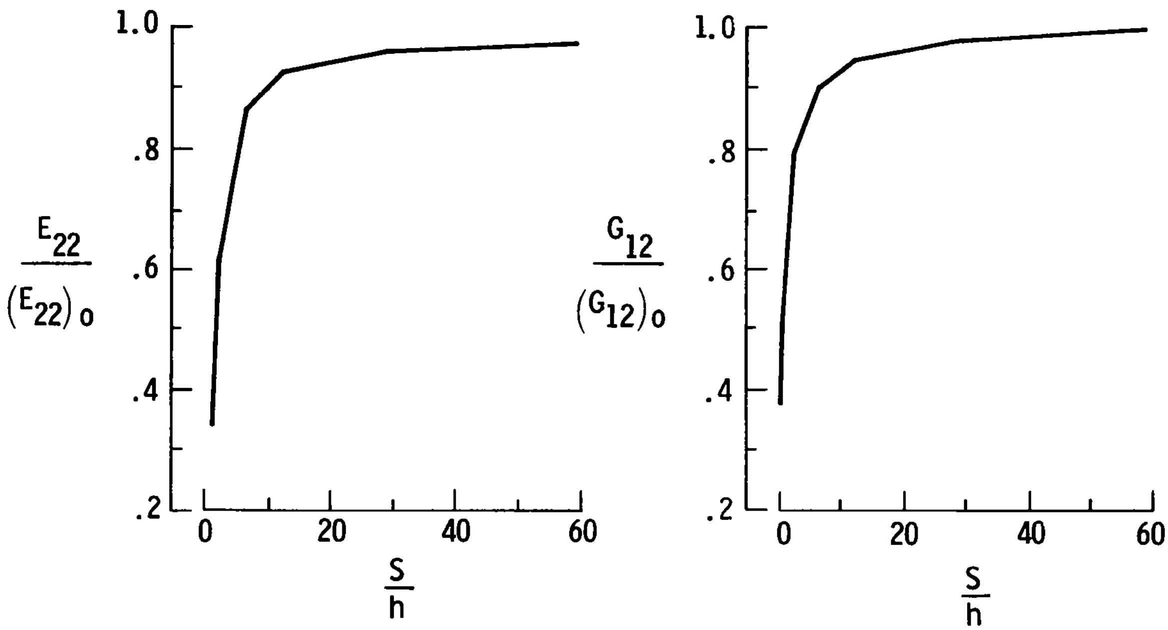

STIFFNESS LOSS DUE TO MATRIX PLY CRACKING

T300 - 5208 GRAPHITE EPOXY

LAYUP	90^0 PLIES		$+45^0$ PLIES		-45^0 PLIES		ΔE_{XX}, %
	$\frac{S}{h}$	$\frac{E_{22}}{(E_{22})_0}$	$\frac{S}{h}$	$\frac{G_{12}}{(G_{12})_0}$	$\frac{S}{h}$	$\frac{G_{12}}{(G_{12})_0}$	
$[0/90]_s$	3.33	65	—	—	—	—	1.2
$[0/\pm 45]_s$	—	—	14.6	95	14.2	95	0.9
$[0/90/\pm 45]_s$	2.37	52	13.6	95	—	—	2.2

STIFFNESS CHANGE WITH DELAMINATION GROWTH

Correlation of delamination size and stiffness shows a much more significant effect on stiffness associated with delamination, which can be rather simply calculated from a modified laminate analysis.

MEASUREMENT OF STIFFNESS CHANGE WITH DELAMINATION GROWTH

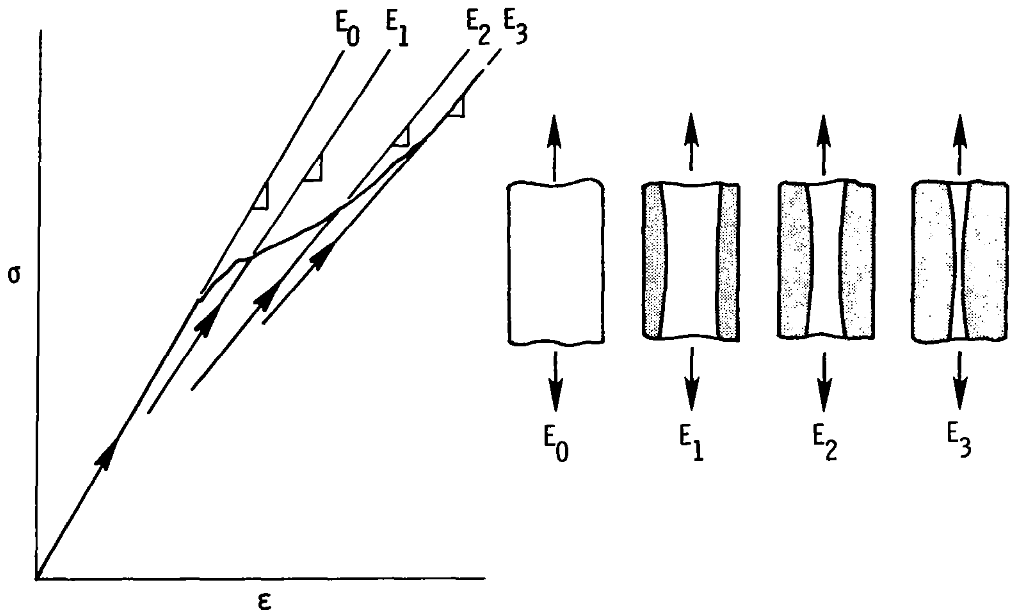

RULE OF MIXTURES ANALYSIS OF STIFFNESS LOSS

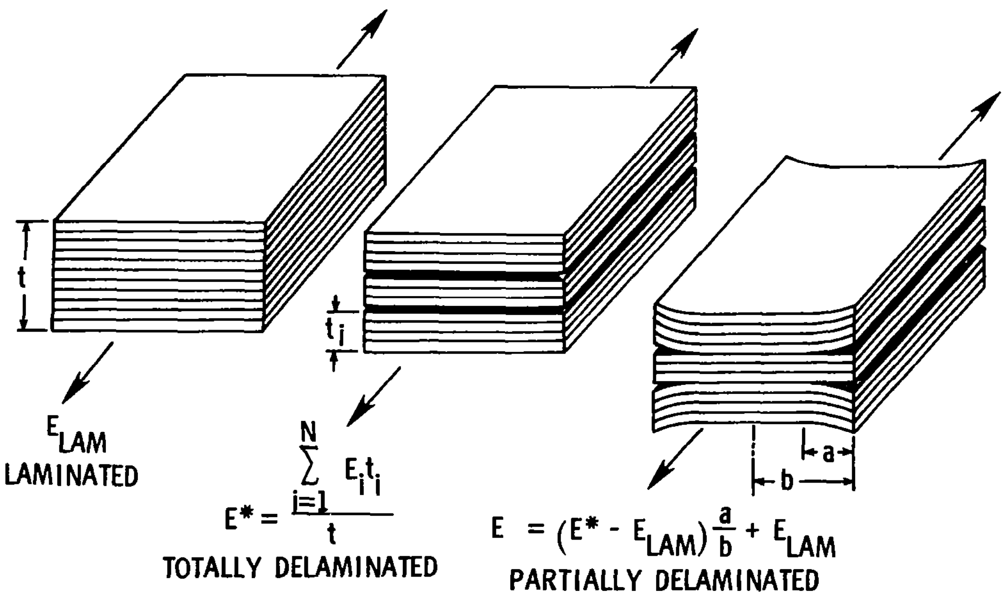

STIFFNESS LOSS AND DELAMINATION SIZE

A comparison between model prediction of stiffness loss and experimental data is given below.

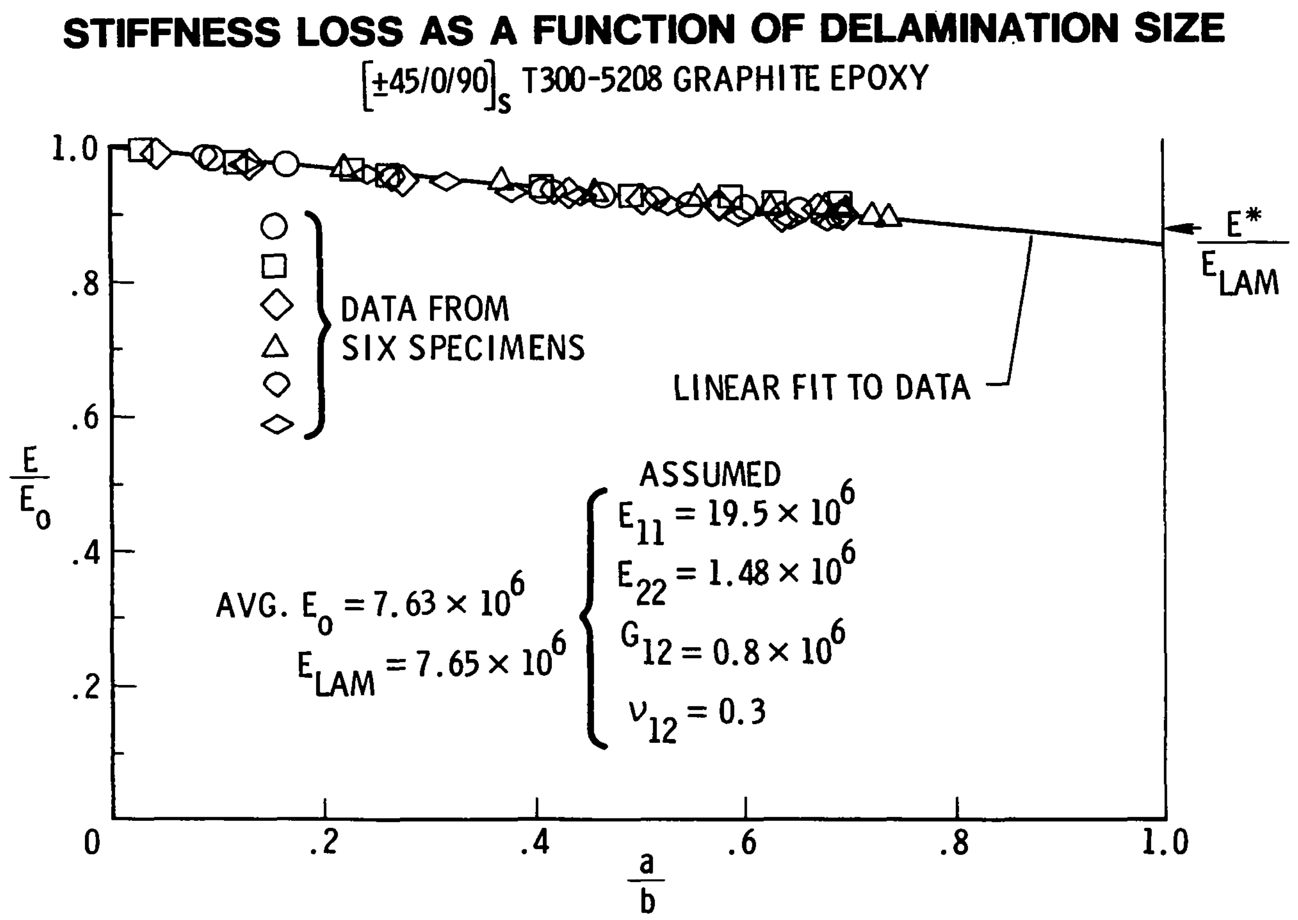

TRANSVERSE-CRACK EXTENSION

Transverse cracking of a ply typically terminates at the interface of a ply of differing orientation. Microscopic and X-ray examination of the crack tip by researchers at VPI&SU and Lockheed, among others, has failed to reveal significant damage to the fibers in the neighboring ply, at least when the specimen has been subjected to only static loading (private communication, K. L. Reifsnider). Recent analysis of the stress concentration and energy release rate associated with the tip of the transverse crack has confirmed the lack of damage potential associated with a transverse ply crack.

The figure below shows the finite-element model discretization of a transverse-ply crack. The ply arrangement for the quasi-isotropic configuration is shown, but three other layups were examined with the same element model. The stress concentration associated with a transverse 90°-ply crack is much less in the quasi-isotropic case than in the transverse $(90)_8$ laminate. This is a result of the relatively small load carried by the cracked ply in the quasi-isotropic laminate. The minimum element size used in this analysis contains approximately 10 fibers. Analysis of stresses with elements on a fiber scale would lose physical meaning, given the homogeneous-ply-stiffness assumptions of the analysis.

LOCAL STRESS CONCENTRATION DUE TO MATRIX CRACK

$[0/90/+45]_s$

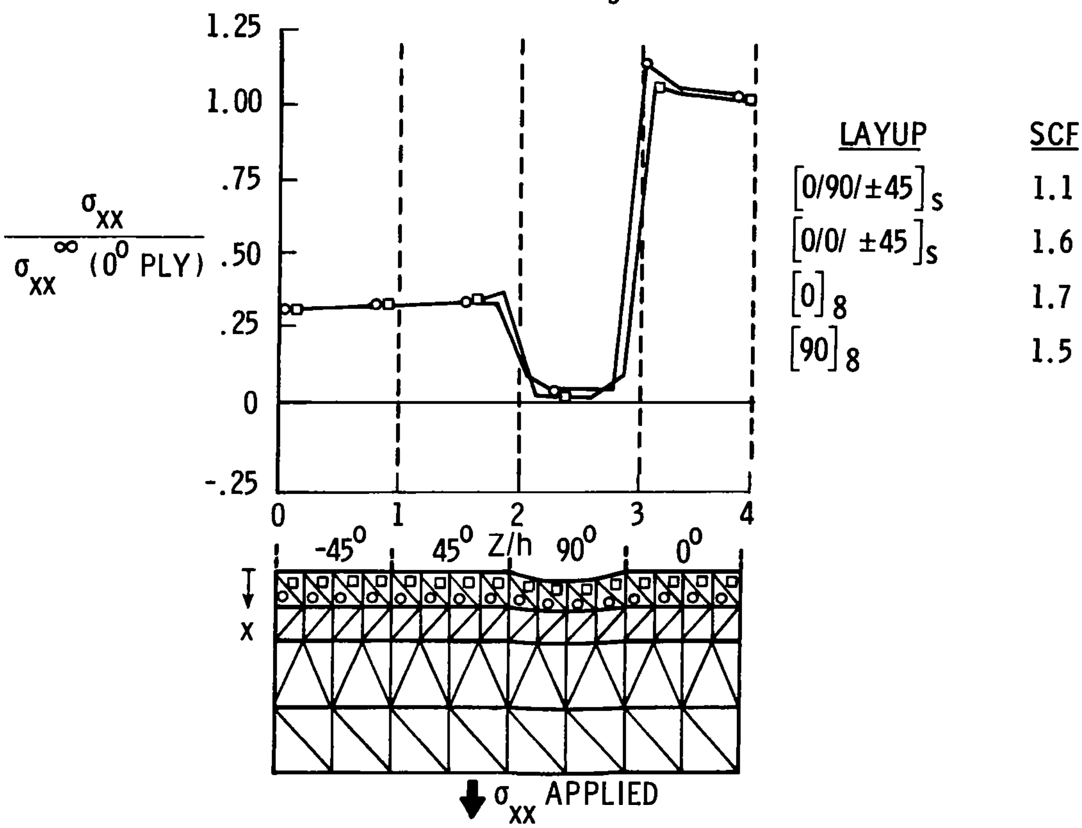

WEIBULL STRENGTH ANALYSIS

Phoenix (ref. 11) has derived a model which can be used to obtain the mean strength of a unidirectional composite as a function of its volume. The volume is given by the product of the number of fibers in cross section (n) and the length divided by the critical length (m). For a typical unidirectional tensile specimen, nm is on the order of 10^6. The figure below shows the characteristic strength distribution function of a single critical length of fiber and the shift of that function associated with a volume of $nm = 10^6$. Taking $W(x) = 0.5$ as the mean strength of a given volume, one can construct a table of strength normalized to a single fiber strength or that of a typical tensile specimen.

CHARACTERISTIC DISTRIBUTION FUNCTION W(x) FOR BUNDLE STRENGTH AND ASSOCIATED WEIBULL APPROXIMATIONS (ref. 11). (ALSO SHOWN IS STRENGTH DISTRIBUTION FOR A BUNDLE WITH 10^6 FIBER ELEMENTS)

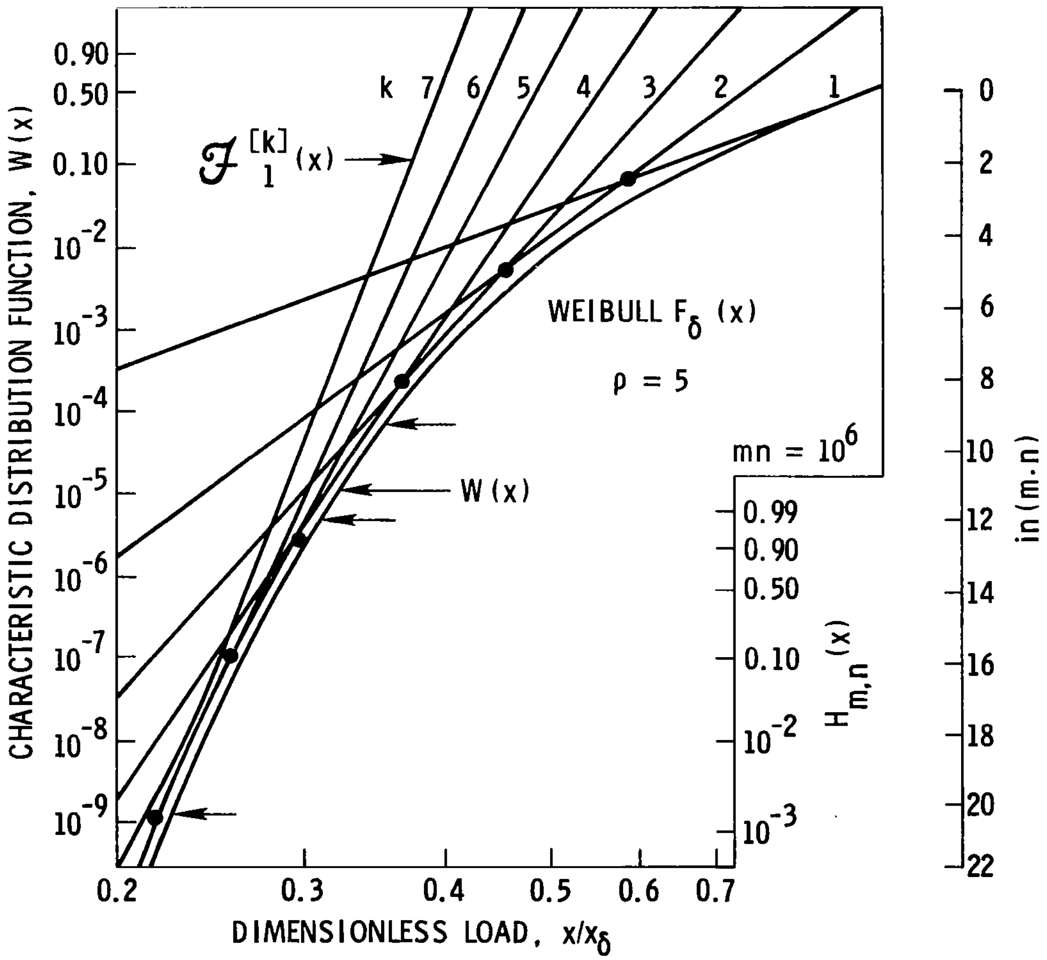

TENSILE STRENGTH VERSUS VOLUME

Given that the stress concentration factor for a transverse crack in a quasi-isotropic laminate is approximately 1.1 and the volume associated with the finite element nearest the transverse crack tip is approximately 5×10^3 in nm units, we can see from the volume dependence of strength derived in the previous table that "failure" of that element is not expected on the basis of the Phoenix theory (ref. 11).

UNDIRECTIONAL TENSILE STRENGTH VS SPECIMEN VOLUME**

CASE	Ln (nxn)	X/X(CASE A)	X/X(CASE B)
A. A single fiber of the critical length	0.0	1.0	4.0
B. A tensile specimen of .080 x .5 x 10. in.	17.9	.25	1.0
C. A single ply .005 in. thick of length .04 in. near tip of transverse crack	9.65	.35	1.4
D. A single layer of fibers of length .04 in. at the tip of the transverse crack	7.13	.41	1.6

** A fiber spacing of .0004 in. and a critical length of .04 in. were assumed.

The figure presented below shows the results of strain energy release rate analysis at the tip of a transverse crack for the geometry shown in the inset. Several types of laminates were analyzed. The energy release rate is plotted as a function of tensile strain. The longitudinal fracture toughness of graphite-epoxy is on the order of 80 to 90 ft-lb/in^2. A transverse crack in a $(0_2/90_2)s$ laminate does not release enough energy to allow the transverse crack to propagate across the 0° ply. Thus the energy release rate analysis approach provides the same prediction of transverse crack stability as the Weibull strength analysis.

STRAIN ENERGY RELEASE RATE ANALYSIS OF MATRIX CRACKS IN EIGHT PLY GRAPHITE EPOXY LAMINATES

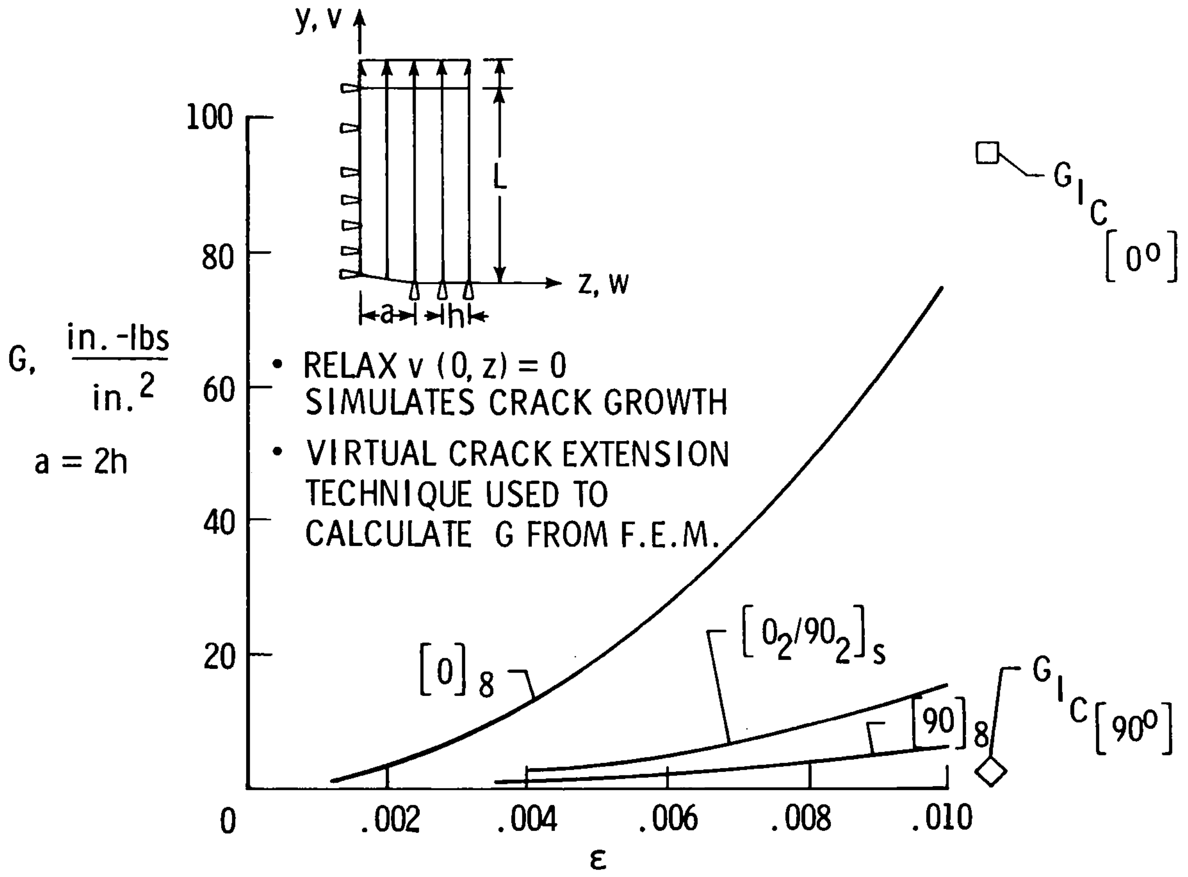

FAILURE BY STRUCTURAL LOAD TRANSFER

The analysis of the final fracture event for tensile-loaded laminates does not appear to depend on the details of ply microcracking. As experimental observations of laminate damage growth under tension have accumulated, the importance of local delaminations in transferring a local load increase to the major load-carrying plies had been postulated by Reifsnider and colleagues (ref. 12). The schematic edge section of laminate damage under static (top) and fatigue (bottom) loading shows regions of the fatigued specimen where essentially all of the applied load must be routed into the 0° plies around regions of extensively delaminated and tranverse-cracked 90° and 45° plies. Prediction of these loads will require more detailed structural modeling.

PREFRACTURE PATTERNS NEAR FRACTURE SITE (ref. 13)

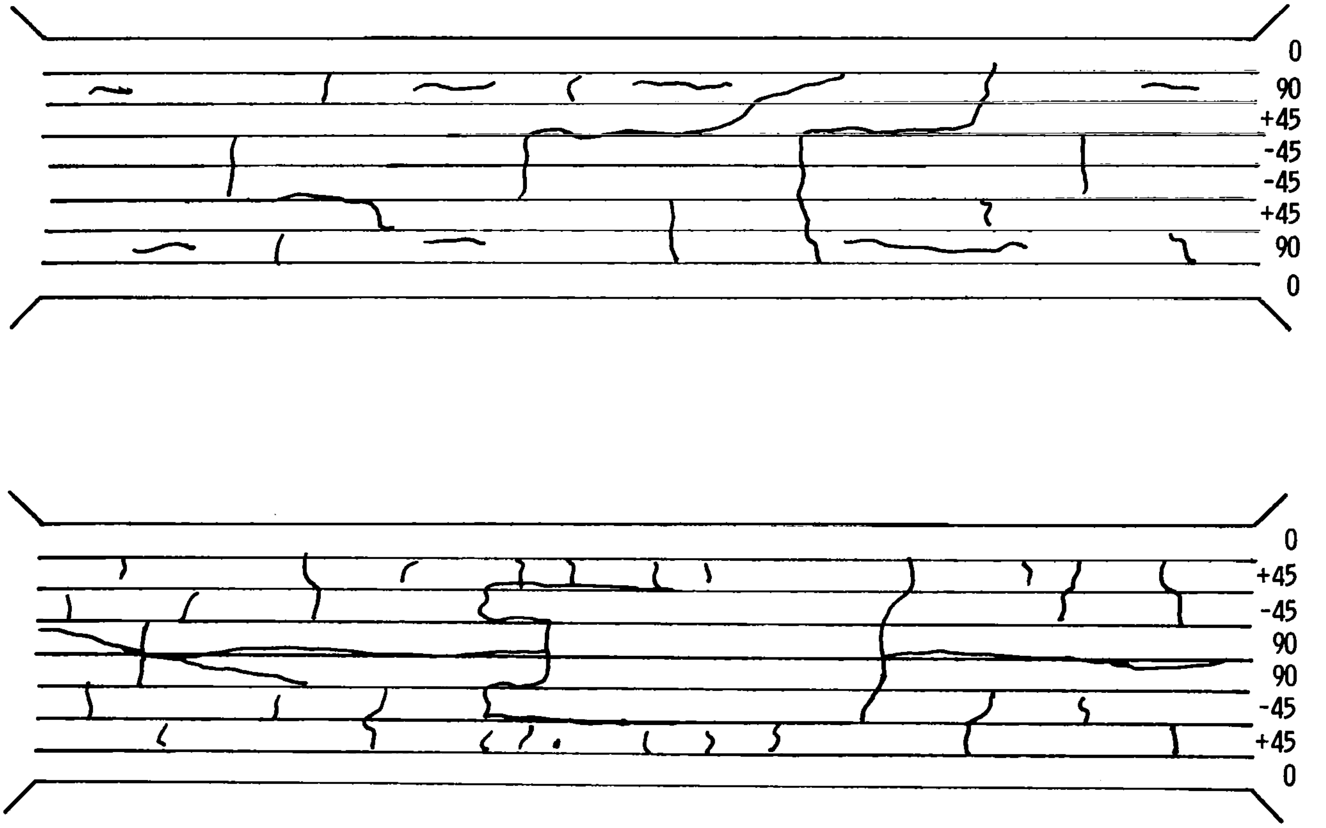

"STRUCTURAL" FAILURE ANALYSIS

The degree to which the details of crack interaction must be modeled to predict tensile failure are being investigated in several ongoing research programs. Structural analysis of composite response can be carried out routinely with numerical methods like finite-element analysis at several different structural levels: microstructural, laminate structural, and macrostructural. However, this does not provide the total solution to fracture analysis of composites. Our understanding of the structural implications of cracking at each level must be improved to provide the proper failure criteria for the structural analysis.

FRACTURE OF STRUCTURAL COMPOSITES

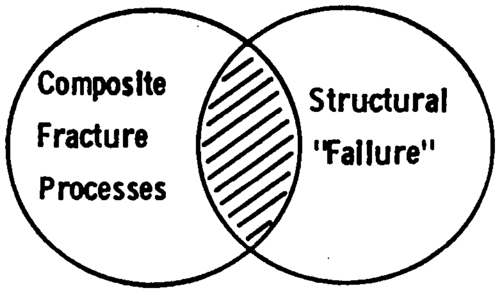

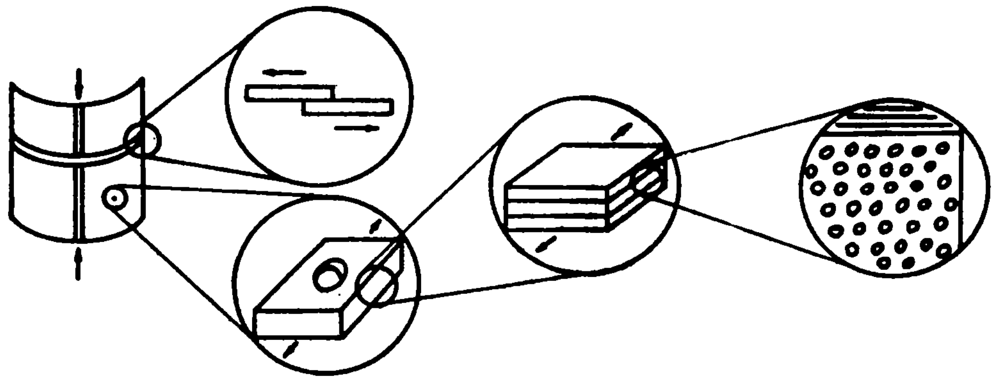

Structural Mechanics	Macro-Mechanics	Mini-Mechanics	Micro-Mechanics
Geometric Imperfections Post-buckling Damage	Local Damage at Stress Concentrations	Ply Fracture Delamination	Fiber Fracture Matrix " Interface "

Fracture ⟺ NDE

What is the significance of damage or defect on the structural integrity?

CONCLUSION AND DISCUSSION

1. Methods of classical fracture mechanics can be viable crack growth criteria for matrix-dominated sublaminate cracks, such as transverse cracking and ply delamination.

2. The energy release rate increases (generally) with the size of crack, which is constrained by the physical dimension of the laminate's ply structure, such as the thickness of the plies. Thus, ply thickness has a profound influence on the growth process of sublaminate cracking, and even on the final failure of the laminate.

3. The finite-element/crack-closure technique is a useful computational tool to simulate sublaminate crack growth, provided the crack paths are relatively simple.

4. The DIB (diiodobutane) enhanced X-radiography is a useful NDE tool for monitoring the growth of sublaminate cracks.

5. For T300/934, the value of G_c is in the range 1.2 to 1.5 in-lb/in^2, but other experiments found it in the range 0.5 to 0.8 (refs. 3 and 6). (See sketch.)

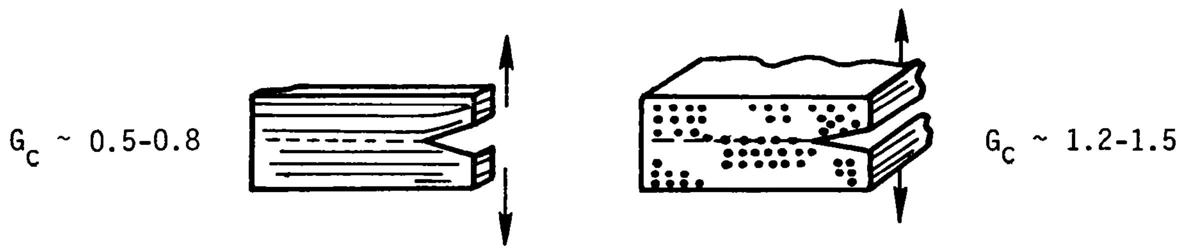

This difference should be verified by additional experimentation.

6. For the best fit of data, the critical material crack size a_c is taken as 0.008 in. This should be verified by micromechanical investigation. Generally, a_c is a function of the size of inhomogeneity (fiber), the stiffness property surrounding the crack, and other processing variables. However, it is not known whether a_c might also depend on the ply structure of the laminate.

7. In the study of delamination, all predictions were based on the total energy release rate $G = G_I + G_{II} + G_{III}$ for both mode-I and mixed-mode cracks. Experimental correlation indicates a need for a mixed-mode crack criterion, such as

$$G_I/G_{Ic} + G_{II}/G_{IIc} + G_{III}/G_{IIIc} = 1$$

There is no firm evidence that G_{IIc} and G_{IIIc} actually exist, and experimental means to measure them independently has not been developed.

8. Some of the observed cracks were actually 'planar cracks'. In the case of a crack front with a complicated contour, the degree to which a 2-D crack growth criterion is readily applicable is not known.

REFERENCES

1. Bjeletich, J. G.; Crossman, F. W.; and Warren, W. J.: The Influence of Stacking Sequence on Failure Modes in Quasi-Isotropic Graphite-Epoxy Laminates. Failure Modes in Composites IV, AIME, 1977, p. 118.

2. Pipes, R. B.; and Pagano, N. J.: Interlaminar Stresses in Composite Laminates Under Uniform Axial Extension. J. Comp. Mater., vol. 4, 1970, p. 538.

3. Crossman, F. W.; Mauri, R. E.; and Warren, W. J.: Hygrothermal Damage Mechanisms in Graphite-Epoxy Composites. NASA CR-3189, 1979.

4. Rodini, B. T.; and Eisenmann, J. R.: An Analytical and Experimental Investigation of Edge Delamination in Composite Laminates. Proc. Fibrous Composites in Structural Design, 1978, p. 441.

5. Reifsnider, K. L. (ed.): Damage in Composite Materials. ASTM STP 775, 1982.

6. Rybicki, E. F.; Schmueser, D. W.; and Fox, J.: An Energy Release Rate Approach for Stable Crack Growth in the Free-Edge Delamination Problem. J. Comp. Mater., vol. 11, 1977, p. 470.

7. Bascom, W. D.; Bitner, J. L.; Moulton, R. J.; and Siebert, A. R.: The Interlaminar Fracture of Organic-Matrix, Woven-Reinforcement Composites. Composites, Jan. 1980, p. 9.

8. Bader, M. G.; and Curtis, P. T.: The Micromechanics of Fibre Composites - Carbon Fibre Programme. Dept. of Metallurgy and Materials Technology, Univ. of Surrey, UK, 1977.

9. Konish, H. J.; Swedlow, J. L.; and Cruse, T. A.: Experimental Investigation of Fracture in an Advanced Fiber Composite. J. Comp. Mater., vol. 6, 1972, p. 114.

10. Scott, J. M.; and Phillips, D. C.: Carbon Fibre Composites With Rubber Toughened Matrices. J. Mater. Sci., vol. 10, 1975, p. 551.

11. Phoenix, S. L.: Statistics for the Strength of Bundles of Fibers in a Matrix. Encyclopedia of Materials Science and Engineering, Pergamon Press, 1981.

12. Reifsnider, K. L.; Stinchcomb, W. W.; Henneke, E. G.; Duke, J., Jr.; and Jamison, R.: Fatigue Damage Strength Relationships in Composite Laminate. Mechanics of Composite Review, 8th Annual (Dayton, Ohio), Air Force Materials Laboratory, 1982.

13. Reifsnider, K. L.; Henneke, E. G.; and Stinchcomb, W. W.: Defect-Property Relationships in a Composite Material. AFML-TR-76-81, Air Force Materials Laboratory, June 1981.

BIBLIOGRAPHY

FREE-EDGE STRESSES

Pipes, R. B., and N. J. Pagano, Interlaminar Stresses in Composite Laminates Under Uniform Axial Extension, J. Comp. Mat., vol. 4, 1970, p. 538.

Pagano, N. J., and R. B. Pipes, The Influence of Stacking Sequence on Laminate Strength, J. Comp. Mat., vol. 5, 1971, p. 50.

Pipes, R. B., and I. M. Daniel, Moire Analysis of the Interlaminar Shear Edge Effect in Laminated Composites, J. Comp. Mat., vol. 6, 1972, p. 62.

Whitney, J. M., and C. E. Browning, Free-Edge Delamination of Tensile Coupons, J. Comp. Mat., vol. 7, 1973, p. 29.

Pagano, N. J., and R. B. Pipes, Some Observations on the Interlaminar Strength of Composite Laminates, Int. J. Mech. Sci., vol. 15, 1973, p. 670.

Pipes, R. B., B. E. Kaminski, and N. J. Pagano, Influence of the Free Edge Upon the Strength of Angle-Ply Laminates, ASTM STP 521, 1973, p. 218.

Whitney, J. M., Free-Edge Effects in the Characterization of Composite Materials, ASTM STP 521, 1973, p. 167.

Pagano, N. J., On the Calculation of Interlaminar Normal Stress in Composite Laminate, J. Comp. Mat., vol. 8, 1974, p. 65.

Barker, R. M., J. R. Dana, and C. W. Pryor, Stress Concentrations Near Holes in Laminates, J. Engineering Mechanics Div., June 1974, p. 477.

Oplinger, D. W., B. S. Parker, and F. P. Chiang, Edge-Effect Studies in Fiber-Reinforced Laminates, Exp. Mech., vol. 14, 1974, p. 347.

Chang, F. H., D. E. Gordon, B. T. Rodini, and R. H. McDaniel, Real-Time Characterization of Damage Growth in Graphite/Epoxy Laminates, J. Comp. Mat., vol. 10, 1976, p. 182.

Renieri, G. D., and C. T. Herakovich, Nonlinear Analysis of Laminated Fibrous Composites, Report No. VPI-E-76-10, Virginia Polytechnic Institute & State University, 1976.

Wang, A. S. D., and F. W. Crossman, Some New Results on Edge Effect in Symmetric Composite Laminates, J. Comp. Mat., vol. 11, 1977, p. 92.

Hsu, P. W., and C. T. Herakovich, Edge Effects in Angle-Ply Composite Laminates, J. Comp. Mat., vol. 11, 1977, p. 422.

Bjeletich, J. G., F. W. Crossman, and W. J. Warren, The Influence of Stacking Sequence on Failure Modes in Quasi-Isotropic Graphite-Epoxy Laminates, Failure Modes in Composites IV, AIME, 1977, p. 118.

Harris, A., and O. Orringer, Investigation of Angle-Ply Delamination Specimen for Interlaminar Strength Test, J. Comp. Mat., vol. 12, 1978, p. 285.

Rybicki, E. F., and D. W. Schmueser, Effect of Stacking Sequence and Lay-up Angle on Free-Edge Stresses Around a Hole in a Laminated Plate Under Tension, J. Comp. Mat., vol. 12, 1978, p. 301.

Wang, S. S., Delamination Fracture From Surface Notch in (45/-45/90/0)s Graphite Epoxy Composites, ICCM2, 1978, p. 277.

Spilker, R. L., and S. C. Chou, Edge Effects in Symmetric Composite Laminates: Importance of Satisfying the Traction-Free-Edge Condition, J. Comp. Mat., vol. 14, 1980, p. 2.

Raju, I. S., J. D. Whitcomb, and J. B. Goree, A New Look at Numerical Analysis of Free-Edge Stresses in Composite Laminates, NASA TN-1751, 1980.

DELAMINATION AND STRAIN ENERGY RELEASE RATE

Rybicki, E. F., D. W. Schmueser, and J. Fox, An Energy Release Rate Approach for Stable Crack Growth in the Free-Edge Delamination Problem, J. Comp. Mat., vol. 11, 1977, p. 470.

Crossman, F. W., R. E. Mauri, and W. J. Warren, Hygrothermal Damage Mechanisms in Graphite-Epoxy Composites, NASA CR-3189, 1979.

Rodini, B. T., and J. R. Eisenmann, An Analytical and Experimental Investigation of Edge Delamination in Composite Laminates, Proc. Fibrous Composites in Structural Design, 1978, p. 441.

Wang, A. S., and F. W. Crossman, Initiation and Growth of Transverse Cracks and Edge Delamination in Composite Laminates, Parts 1 and 2, J. Comp. Mat., Supplemental vol. 14, 1980, p. 72.

Wang, A. S. D., Growth Mechanisms of Transverse Cracks and Ply Delamination in Composite Laminates, ICCM3, 1980, p. 170.

Crossman, R. W., and A. S. D. Wang, The Dependence of Transverse Cracking and Delamination on Ply Thickness in Graphite/Epoxy Laminates, ASTM STP 775, 1982, pp. 118-139.

Law, G. E., Fracture Analysis of (25/-25/90n)s Graphite-Epoxy Composite Laminates, Ph. D. Dissertation, Drexel University, June 1981.

Wilkins, D. J., J. R. Eisenmann, R. A. Camin, W. S. Margolis, and R. A. Benson, Characterizing Delamination Growth in Graphite Epoxy, ASTM STP 775, 1982, pp. 168-183.

O'Brien, T. K., Characterization of Delamination Onset and Growth in a Composite Laminate, ASTM STP 775, 1982, pp. 140-167.

Williams, D. R., Mode I Transverse Cracking in an Epoxy and Graphite Fiber Reinforced Epoxy, M. S. Thesis, Texas A&M University, Report No. MM 3724-81-16, Dec. 1981.

Cullen, J. S., Mode I Delamination of Unidirectional Graphite/Epoxy Composite Under Complex Load Histories, M. S. Thesis, Texas A&M Univ., report no. MM 3724-81-13, Dec. 1981.

Vanderkley, P. S., Mode I-Mode II Delamination Fracture Toughness of a Unidirectional Graphite/Epoxy Composite, M. S. Thesis, Texas A&M Univ., report no. MM 3724-81-15, Dec. 1981.

Early, J. W., Compression Induced Delamination in a Unidirectional Graphite/Epoxy Composite, M. S. Thesis, Texas A&M Univ., report no. MM 3724-81-14, Dec. 1981.

IMPROVING THE INTERLAMINAR TOUGHNESS OF COMPOSITES

Scott, J. M., and D. C. Phillips, Carbon Fibre Composites With Rubber Toughened Matrices, J. Mat. Sci., vol. 10, 1975, p. 551.

Bascom, W. D., R. L. Cottington, and C. O. Timmons, Fracture Design Criteria for Structural Adhesive Bonding: Promise and Problems, Naval Engineers J., Aug. 1976, p. 73.

Bascom, W. D., J. L. Bitner, R. J. Moulton, and A. R. Siebert, The Interlaminar Fracture of Organic-Matrix, Woven Reinforcement Composites, Composites, Jan. 1980, p. 9.

Miller, A. G., P. E. Hertzberg, and V. W. Rantala, Toughness Testing of Composite Materials, SAMPE Quarterly, Jan. 1981, p. 36.

THE INFLUENCE OF DELAMINATION OF COMPOSITE FAILURE

Mulville, D. R., and I. Wollock, Failure of Polymer Composites, in Developments in Polymer Fracture I, E. H. Andrews, ed., chapter 8, Applied Science Pub., London, 1979.

Reifsnider, K. L., E. G. Henneke, and W. W. Stinchcomb, Defect-Property Relationships in Composite Materials, AFML-TR-76-81, Air Force Materials Laboratory, June 1981.

Reifsnider, K. L., Mechanics of Failure of Composite Materials, presented at Fracture Mechanics Symposium, Charlottesville, NC, 1978 (Navy Structural Mechanics Series).

O'Brien, T. K., The Effect of Delamination on the Tensile Strength of Unnotched, Quasi-Isotropic, Graphite/Epoxy Laminates, Proc. SESA/JSME Conf., Hawaii, May 1982.

Stinchcomb, W. W., K. L. Reifsnider, P. Young, and M. N. Gibbons, Investigation and Characterization of Constraint Effects on Flaw Growth During Fatigue Loading of Composite Materials, Final Report on NASA Grant NSG-1364, June 1979.

Kim, R. Y., Experimental Assessment of Static and Fatigue Damage of Graphite/Epoxy Laminates, ICCM3, 1980, p. 1015.

Reifsnider, K. L., and A. Tulag, Analysis of Fatigue Damage in Composite Laminates, Int. J. Fatigue, Jan. 1980, p. 3.

Reifsnider, K. L., The Effect of Lamination-Induced Stresses on Fatigue Damage Development at Internal Flaws, Comp. Tech. Rev., vol. 3, 1981, p. 17.

Batdorf, S. B., Tensile Strength of Unidirectionally Reinforced Composites, Part I, J. Reinforced Plast. & Comp., To be published in 1982.

Phoenix, S. L., Statistics for the Strength of Bundles of Fibers in a Matrix, Encyclopedia of Materials Science and Engineering, Pergamon Press, 1981.

Smith, R. L., A Probability Model for Fibrous Composites with Local Load-Sharing, Proc. Roy. Soc. London Ser. A-372, p. 539.

FRACTURE MECHANICS

Zweben, C., Fracture Mechanics and Composite Materials: A Critical Analysis, ASTM STP 521, 1973, p. 65.

Kanninen, M. F., E. F. Rybicki, and H. F. Brinson, A Critical Look at Current Applications of Fracture Mechanics to the Failure of Fibre-Reinforced Composites, Composites, Jan. 1977, p. 17.

Waddoups, M. E., J. R. Eisenmann, and B. E. Kaminski, Macroscopic Fracture Mechanics of Advanced Composite Materials, J. Comp. Mat., vol. 5, 1971, p. 164.

Konish, H. J., J. L. Swedlow, and T. A. Cruse, Experimental Investigation of Fracture in an Advanced Fiber Composite, J. Comp. Mat., vol. 6, 1972, p. 114.

Cruse, T. A., and M. G. Stout, Fractographic Study of Graphite-Epoxy Laminated Fracture Specimens, J. Comp. Mat., vol. 7, 1973, p. 200.

Mandell, J. F., S. S. Wang, and F. J. McGarry, The Extension of Crack Tip Damage Zones in Fiber Reinforced Plastic Laminates, J. Comp. Mat., vol. 9, 1975, p. 266.

Altus, E., and A. Rotem, A 3-D Fracture Mechanics Approach to the Strength of Composite Materials, Eng. Fracture Mech., vol. 14, 1981, p. 637.